HHS Public Access

Author manuscript

Cell. Author manuscript; available in PMC 2023 January 20.

Published in final edited form as:

Cell. 2022 January 20; 185(2): 328–344.e26. doi:10.1016/j.cell.2021.12.014.

Control of mammalian locomotion by ventral spinocerebellar tract neurons

Joshua I. Chalif[1,2,‡], **María de Lourdes Martínez-Silva**[1,2], **John G. Pagiazitis**[1,2], **Andrew J. Murray**[4], **George Z. Mentis**[1,2,3,*]

[1]Center for Motor Neuron Biology and Disease, Columbia University, New York, NY 10032, USA

[2]Dept. of Neurology, Columbia University, New York, NY 10032, USA

[3]Dept. of Pathology and Cell Biology, Columbia University, New York, NY 10032, USA

[4]Sainsbury Wellcome Centre, University College London, 25 Howland Street, London W1T 4JG, UK

Summary

Locomotion is a complex behavior required for animal survival. Vertebrate locomotion depends on spinal interneurons termed the central pattern generator (CPG), which generates activity responsible for the alternation of flexor and extensor muscles and the left and right side of the body. It is unknown whether multiple or a single neuronal type is responsible for the control of mammalian locomotion. Here, we show that ventral spinocerebellar tract neurons (VSCTs) drive generation and maintenance of locomotor behavior in neonatal and adult mice. Using mouse genetics, physiological, anatomical and behavioral assays, we demonstrate that VSCTs exhibit rhythmogenic properties and neuronal circuit connectivity consistent with their essential role in the locomotor CPG. Importantly, optogenetic activation and chemogenetic silencing reveals that VSCTs are necessary and sufficient for locomotion. These findings identify VSCTs as critical components for mammalian locomotion and provide a paradigm shift in our understanding of neural control of complex behaviors.

In brief

Ventral spinocerebellar tract neurons (VSCTs) are necessary and sufficient to drive generation and maintenance of locomotor behavior in mice.

*Corresponding author & Lead contact: Tel: +1-212-305-9846, gzmentis@columbia.edu.
‡current address: Dept. of Neurosurgery, Brigham and Women's Hospital, Boston, MA 02115, USA

Author Contributions:
GZM conceived project. JIC and GZM designed experiments. JIC, MLMS, JGP conducted experiments and analyzed data. AJM produced the rabies viruses, assist with analysis and interpretation of results. GZM contributed in some experiments and analysis. JIC and GZM wrote the manuscript with input from all authors.

Declaration of Interests:
The authors declare no competing interests.

Inclusion and diversity statement:
One or more of the authors of this paper self-identifies as an underrepresented ethnic minority in science.

Graphical Abstract

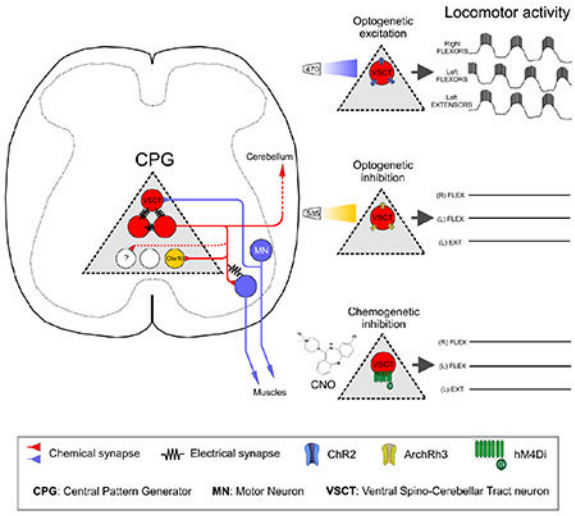

Introduction

Locomotion is an essential animal behavior that is critical for survival. Overground locomotion is defined as the alternating, rhythmic motor activity between opposing limbs as well as between antagonistic muscles of the same limb. While sensory feedback and supraspinal commands are important for modulating locomotion, a network of spinal interneurons - known as the central pattern generator (CPG) - is thought to be responsible for the genesis of locomotor activity (Guertin, 2012; Kiehn, 2016) without relying on sensory or descending inputs (Graham Brown, 1911). These neurons are thought to activate spinal motor neurons (MNs) in a patterned manner. Subsequently, MNs convey their motor commands to peripheral muscles, resulting in limb movement. Recent studies have begun to unravel the organization of the spinal neuronal circuits underlying left-right and flexor-extensor alternation (Crone et al., 2008; Gosgnach et al., 2006; Talpalar et al., 2013; Zhang et al., 2014), demonstrating the modularity and speed-dependency of these circuits. However, it is unknown whether a single neuronal population is necessary and sufficient for the generation and maintenance of locomotor activity. Here, using mice as an experimental model, we identify ventral spinocerebellar tract neurons (VSCTs) as an essential population of spinal neurons for mammalian locomotion.

In rodents, locomotor behavior is evident at early postnatal periods, since intact *ex vivo* spinal cord preparations can produce locomotor-like behavior following sensory fiber stimulation or application of a cocktail of drugs (Mentis et al., 2005; Talpalar et al., 2013; Whelan et al., 2000). This behavior is characterized by alternating rhythmic oscillations of MN activity between the left and right sides of the spinal cord and between rostral (L1/L2) and caudal (L4/L5) lumbar segments (Bonnot et al., 2002). Traditionally, CPG networks are thought to reside upstream of MNs (Goulding and Pfaff, 2005; Kiehn and Butt, 2003), while MNs act as the spinal output to convey motor commands to muscles. However, we have previously shown that stimulation of MN axons results in locomotor

activity (Mentis et al., 2005). Additionally, manipulation of MN activity can alter ongoing locomotor behavior (Falgairolle et al., 2017) and zebrafish MNs can influence premotor excitatory CPG elements (Song et al., 2016). These observations implicate MNs in the regulation of locomotor rhythmogenesis via a local spinal neuron that is activated by MN axon collaterals. Although previous studies have provided evidence that the neural circuits encompassing CPG elements reside in the ventral spinal cord (Grillner and Wallén, 1985; Kiehn, 2016), the only spinal neurons that are contacted by MN axon collaterals known to date are Renshaw cells (Alvarez and Fyffe, 2007; Eccles et al., 1954; Mentis et al., 2005; Renshaw, 1946) and $Sim1^+$ interneurons (Chopek et al., 2018). However, Renshaw cells do not affect the locomotor CPG (Enjin et al., 2017; Noga et al., 1987) and $Sim1^+$ neurons regulate the speed of vertebrate locomotion and contribute to vigor and coordination, but are not involved in locomotor rhythmogenesis (Zhang et al., 2008). Thus, MNs may contact another yet-to-be-defined neuron that resides within the ventral spinal cord and mediates locomotor rhythmogenesis.

Here, we show that ventral spinocerebellar tract (VSCT) neurons are contacted by MN axon collaterals during early development via both chemical and electrical synapses. The nature of these contacts is both chemical via excitatory synapses as well as electrical through gap junctions. Furthermore, VSCTs possess functional intrinsic properties consistent with a role in locomotor rhythmogenesis. We demonstrate that VSCTs contain axon collaterals that form local circuits with spinal MNs and at least $Chx10^+$ spinal neurons. Importantly, optogenetic activation and chemogenetic silencing of VSCTs reveals that VSCT neurons are both necessary and sufficient to produce locomotor behavior during postnatal development. Finally, chemogenetic silencing of VSCTs in freely moving adult mice perturbs their locomotor ability.

Results

VSCTs are activated monosynaptically and electrically by motor neurons.

To investigate whether spinal MNs activate a yet-unknown interneuron, we unbiasedly examined the activity of spinal neurons through two-photon (2P) calcium imaging in the intact *ex vivo* mouse spinal cord at postnatal day 4 (P4). Spinal neurons were indiscriminately labelled with Calcium Green 1 by electroporation (Fig. S1A,B and Methods). Stimulation of the ventral root (VR) revealed increases in fluorescence in interneurons located dorsolateral to the MN nucleus (Fig. S1C,D). Visually-guided, whole-cell patch clamp recordings revealed that these neurons displayed graded excitatory postsynaptic potentials (EPSPs) with a short latency following VR stimulation (Fig. S1E), indicating that can be activated directly by MN axon collaterals. These neurons, located in the dorsal aspect of the MN nucleus were reminiscent of spinal border cells - a subset of VSCTs (Bras et al., 1988; Cooper and Sherrington, 1940). To determine whether these neurons were VSCTs, the tracer cholera toxin subunit b conjugated to Alexa-555 (CTb-555) was injected into the cerebellum in mice at P0 (Fig. 1A). At P4, the injection was verified to be specific to the cerebellum (Fig. S1F), as shown by CTb signal only in the cerebellum (Fig. S1G). Individual VSCTs located in the L1/2 spinal segments were then visually targeted for whole-cell patch clamp recordings guided by 2P laser microscopy (Fig. 1B,C)

utilizing the *ex vivo* cerebellum-brainstem-spinal cord preparation. Only a single VSCT was recorded per spinal cord, targeted from the lateral aspect. In addition to co-localization of CTb-555 with the intracellular dye (Fig. 1C), the identity of VSCTs was further demonstrated by the presence of an all-or-none antidromic action potential (AP) following cerebellum stimulation (Fig. 1D–F). VSCTs exhibited higher excitability compared to MNs (Fletcher et al., 2017) (Fig. 1G–K) despite having a soma size similar to MNs (Fletcher et al., 2017) (Fig. 1L).

We next sought to identify the major source of synaptic activation of VSCTs. A major source of afferents originates from the periphery and sensory fiber stimulation can activate locomotor networks (Whelan et al., 2000). Thus, we tested whether dorsal root (DR) stimulation, including proprioceptors, could activate VSCTs. Stimulation of the homo-segmental DR revealed monosynaptically-evoked EPSPs in 40% of VSCTs (6/15) at P3-P5 (Fig. 2A). Monosynapticity was determined by the absence of a change in the coefficient of variation (CV) of the latency of the response onset at different stimulation frequencies (0.1-10Hz) as we reported (Mendelsohn et al., 2015) (Fig. 2B,C). Staining with Parvalbumin (Pv) and vesicular glutamate transporter 1 (VGluT1) antibodies confirmed apposition of proprioceptive synapses on VSCTs (Fig. 2,I). To quantify the number of VSCTs receiving proprioceptive synapses, VSCTs were labelled with CTb555 from cerebellum injection at birth. At P4/P5, DR L1 sensory fibers using the *ex vivo* spinal cord preparation were labelled orthogradely with Cascade Blue Dextran and subsequently marked with VGluT1 and Parvalbumin. The presence of VGluT1, Parvalbumin and Dextran has been demonstrated to label selectively proprioceptive synapses (Chen et al., 2006; Mentis et al., 2011; Mentis et al., 2006). We found that 8 VSCTs (~47%, 8/17, N=6 mice) receive proprioceptive synapses on their soma or proximal dendrites (Fig. S1H–J), while 9 VSCTs (~53%, 9/17, N=6 mice) did not. These results are in agreement with our physiological studies and demonstrate that ~45% of VSCTs receive proprioceptive synapses.

We next examined whether VSCTs could be activated directly by MN axon collaterals. Utilizing the *ex vivo* spinal cord preparation (P3-P5), intracellular recordings of VSCTs (Fig. 1C) exhibited short latency, depolarizing and graded EPSPs sufficient to induce APs following VR stimulation (Fig. 2D). All VSCTs (n=10) were activated monosynaptically since different frequencies of VR stimulation (0.1-10Hz) resulted in no change in the CV of the latency of the onset of EPSPs (Fig. 2E,F). These EPSPs decreased at more depolarized holding potentials indicating the involvement of chemical synapses (Fig. S1K,L). Through the addition of mecamylamine (cholinergic receptor blocker) and NBQX (glutamatergic receptor blocker), we determined that MNs activate VSCTs directly via both cholinergic and glutamatergic receptors (Fig. 2G,H). Surprisingly, a residual component was evident following both cholinergic and glutamatergic blockade in VSCTs, which was blocked after exposure to carbenoxolone (gap junction blocker), indicating that MNs and VSCTs are also electrically coupled (Fig. 2G,H). To evaluate the spread of current from the entire population of spinocerebellar tract neurons (SCTs) to a population of MNs located within one spinal segment, we utilized the cerebellum-brainstem-spinal cord *ex vivo* preparation at P4-P5 (Fig. S2A–C). Maximal cerebellum activation resulted in robust VR responses with a latency of ~40ms (Fig. S2C), consistent with the latency of the antidromic AP of VSCTs from the cerebellum (Fig. 1E). Comparison of the VR response following

cerebellar stimulation to that from the homonymous DR (Fig. S2B,C) revealed that cerebellar stimulation resulted in ~35% of the MN activation compared to DR stimulation (Fig. S2D,E). This indicates robust activation of MNs by axon collaterals from SCTs. The VR response was monosynaptic in nature since stimulation at different frequencies resulted in an identical latency, indicative of monosynapticity (Fig. S2F). By measuring the VR response following cerebellum stimulation under carbenoxolone exposure (100μM) we found a significant, yet modest ~15% reduction of the VR response (Fig. S2G,H). Further exposure to NBQX (20μM) and APV (100μM) (non-NMDA and NMDA glutamate receptor blockers respectively), abolished the VR response (Fig. S2G,H). These results indicate that the spread of current through gaps junctions from SCTs to MNs is minimal and the chemical nature of communication between VSCTs and MNs is dominant.

The nature of MN-to-VSCT synaptic transmission was further investigated by morphological analysis in which MN axon collaterals were found to form cholinergic synapses on VSCTs (Fig. 2,J–L). The electrical communication between VSCTs and MNs was also established morphologically. During intracellular recordings, Neurobiotin (in intracellular electrode) was allowed to diffuse into the recorded neuron as to reveal its somato-dendritic morphology and axonal trajectory. However, Neurobiotin is also a tracer known to cross gap junctions (Pastor et al., 2003) and identify dye-coupled partners of the recorded neuron. In this manner, we observed Neurobiotin-labeled MNs following a single VSCT fill (Fig. S2I,J), and dye coupling was also observed amongst VSCTs (Fig. S2K). Seven VSCTs (~60%, 7/12) were dye coupled, three of which exhibited dye coupling only amongst other VSCTs, whereas three more VSCTs exhibited dye coupling with both other VSCTs and MNs. One VSCT was dye-coupled only with MNs. Despite dye coupling underestimates the extent of electrical coupling due to limitations in the time and diffusion rate of the tracer, our results indicate a substantial degree of electrical coupling (>60%) for VSCTs.

Taken together, these experiments demonstrate that MNs activate VSCTs via both chemical and electrical synapses. They also reveal the electrical communication amongst VSCTs themselves.

VSCTs are rhythmically active during locomotor-like behavior

Lundberg postulated that VSCTs relay information about the activity of spinal networks to the cerebellum (Lundberg, 1971). This hypothesis gained traction from experiments in adult cats demonstrating that the activity of VSCTs is rhythmically modulated during locomotion after deafferentation (Arshavsky et al., 1972). To test whether VSCTs are rhythmically active during locomotor behavior, we induced locomotor-like activity utilizing the intact *ex vivo* mouse spinal cord (from T4 to *cauda equina*) as previously reported (Bonnot et al., 2002; Jiang et al., 1999). Stimulation of lumbar VRs or DRs (Mentis et al., 2005) while recording intracellularly from individual VSCTs (located in the L1/L2 segments) concomitantly with the left and right L1 VRs and the right (or left) L5 VR. VSCTs (n=6) displayed robust rhythmic behavior and bouts of APs (Fig. 3A) in phase with the ipsilateral, homosegmental L1 VR (containing predominately-flexor MNs). Two more VSCTs exhibited

sub-threshold rhythmic oscillations during sensory-induced locomotor behavior (n=2; Fig. S3A).

Calculation of the timing of the onset of VSCT firing compared to the onset of the flexor burst, normalized to the locomotor cycle length, revealed the relationship between the initiation of VSCT firing and that of MN firing in the same spinal segment for each locomotor cycle (Fig. $3B_1$ and see Methods). The mean vector value from each of the individual VSCTs, plotted in a circular plot corresponding to the locomotor cycle (Fig. $3B_2$), determined if the combined population of VSCTs exhibited rhythmic activity. On average, we found that VSCTs elicited their first AP preceding the onset of the cycle from the homosegmental VR (Fig. $3B_{1,2}$ and Fig. S3B and Methods). Thus, VSCTs fire rhythmically with flexor MNs and elicit APs prior to the locomotor cycle exhibited by homosegmental MNs.

VSCTs exhibit rhythmogenic characteristics

We observed that VSCTs exhibited a pacemaker current, a rhythmogenic property characterized by a slow, steady depolarization until the threshold voltage for AP induction is reached both spontaneously (Fig. 3C) and evoked (Fig. 3D). The H-current (I_h) is caused by the opening of a non-selective cation channel with an equilibrium potential of −35mV and is known to underlie pacemaker currents in neurons (Lüthi and McCormick, 1998). VSCTs displayed the characteristic voltage sag and post-inhibitory rebound in response to a negative current injection, indicative of the presence of I_h (Fig. 3E). The sag and post-inhibitory rebound were both time-dependent and voltage-dependent (Fig. S3C,D). The post-inhibitory rebound was large enough to cause VSCTs to fire an AP from their own resting membrane potential (Fig. 3E and Fig. S3C,D). Both sag and post-inhibitory rebound were abolished by bath application of ZD7288 – a selective blocker of I_h(Rothberg et al., 2002) - and recovered upon washout (Fig. 3E–G). ZD7288 decreased the resting membrane potential of VSCTs, increased their excitability, and did not affect the threshold voltage for AP induction (Fig. S3E–J) as expected (Kase and Imoto, 2012; Lüthi and McCormick, 1998). Taken together, the electrical coupling between VSCTs and the presence of the pacemaker h-current may underlie the contribution of VSCTs to locomotor rhythmogenesis.

VSCTs are necessary and sufficient for locomotor rhythmogenesis during early postnatal development

To address the functional involvement of VSCTs in locomotor behavior, we used viral-mediated gene delivery to selectively manipulate neuronal activity of SCTs. Cerebellum injection with canine adenovirus 2 (CAV2) expressing GFP demonstrated effective and specific transduction of SCTs (Fig. 4M). The efficiency of VSCTs transduction by CAV2-GFP-CRE was ~60% (Fig. 4N and Fig. S4A,B) when compared with CTb-555 co-injected to cerebellum at P0/1 and examined at P4/5. To activate VSCTs, CAV2-GFP-CRE, CAV2-CRE or CAV2-GFP was injected into the cerebellum of /*s*/-Channelrhodopsin2 mice at P0. We then used the *ex vivo* spinal cord preparation (T4-*cauda equina*) at P4 and 470nm light - delivered through a LED – to photoactivate VSCTs bilaterally in the L1/L2 lumbar segments (Fig. 4A), considered as the most rhythmogenic spinal cord area (Cazalets et al., 1995; Kjaerulff and Kiehn, 1996). Remarkably, VSCT photoactivation produced robust

locomotor-like behavior in all preparations (N=8) (Fig. 4B,C). Dorsal spinocerebellar tract neurons' (DSCTs) illumination from the dorsal aspect in the same preparations (flipped over 180°, Fig. 4D), revealed no effects (Fig. 4E,F). The same preparations (N=8) were flipped over once more to activate VSCTs, resulting in robust locomotor behavior and indicating that VSCTs, but not DSCTs, were responsible for locomotor behavior. Morphological experiments revealed the presence of ~1200 DSCTs (Fig. S4C,D) and ~850 VSCTs (Fig. S4C,E) in the L1 spinal segment at P4. In control experiments, LED illumination had no effects on VSCTs expressing CAV2-GFP (Fig. S4F–H). Using a distinct approach, ChR2 was introduced to SCTs by a rabies virus (N2C) expressing both ChR2 and YFP as previously reported (Reardon et al., 2016). The virus was injected into the cerebellum in wild type (WT) mice at P0 and experiments were performed at P4-P5 using the ex vivo spinal cord to photoactivate VSCTs from the ventral side with a 470nm LED. This approach also produced robust locomotor-like activity with similar locomotor frequencies (Fig. S5A–C) to those observed when CAV2-CRE injected in/*s*/-ChR2 mice. Importantly, the frequency of the induced locomotor rhythm following photoactivation of VSCTs was similar to that produced after sensory or MN axon stimulation, and faster than that produced via application of a pharmacological cocktail (Fig. 4O). Together, these results demonstrate that activation of VSCTs is sufficient to elicit locomotor behavior.

Archaerhodopsin-3 (ArchR3) was introduced to VSCTs by injection of CAV2-GFP-CRE (or CAV2-GFP) into the cerebellum of/*s*/-ArchR3 mice at P0 (Fig. S5D) to silence VSCTs during sensory-evoked locomotor activity to reveal whether VSCTs are necessary for locomotor behavior. Utilizing the *ex vivo* spinal cord preparation, we photo-silenced VSCTs through illumination with a 585nm LED light delivered to the L1/L2 segments ventrally and bilaterally (Fig. S5E,F) at P3-P5, which resulted in severe degradation of locomotor activity (Fig. S5G,H). To increase the number of silenced VSCTs beyond those neurons located in L1/L2 segments, we next used a chemogenetic approach by injecting CAV2-GFP-CRE or CAV2-GFP at P0 into the cerebellum of mice with a floxed inhibitory designer receptor exclusively activated by designer drugs (DREADDs; hM4Di) (Fig. 4M,N). Strikingly, bath application of clozapine N-oxide (CNO; 10μM) to silence SCTs throughout the spinal cord prevented the induction of locomotor-like activity following either sensory stimulation (Fig. 4G,H) or MN axon stimulation (Fig. 4I,J). The effect was reversible because locomotor activity resumed ~30min after CNO washout and following stimulation of either sensory fibers in a DR (Fig. 4G) or MN axons in a VR (Fig. 4I). Importantly, exposure to CNO did not affect glutamatergic neurotransmission as shown by the unchanged amplitude of the homosegmental monosynaptic DR-to-VR reflex (Fig. S5I,J), indicating that MNs function normally. Exposure to CNO in mice injected with CAV2-GFP had no effect on the locomotor frequency induced by DR or VR stimulation as expected (Fig. S5K,L). Thus, these experiments indicate that VSCTs are necessary for the induction of locomotor activity.

Silencing of SCTs through CNO exposure during ongoing locomotor-like activity induced by a cocktail of drugs (NMDA, serotonin, and dopamine) (Fig. 4K,L), known to produce locomotor behavior in neonates (Bonnot et al., 2002; Mentis et al., 2005) abolished the activity shortly after CNO exposure, providing evidence that VSCTs are necessary not only for the induction of locomotor behavior but also for its maintenance (Fig. 4K,L). In

sum, these experiments demonstrate that VSCTs are necessary and sufficient to induce and maintain locomotor behavior during mouse development.

I_h current and electrical coupling in VSCTs mediate locomotor rhythmogenesis

Since VSCTs exhibit an I_h current, we investigated whether I_h is necessary to produce locomotor activity following photoactivation of VSCTs. This was compared side-by-side to locomotor activity induced by DR stimulation. VSCTs were transduced with by CAV2-GFP-CRE in/*s*/-ChR2 mice at P0. We then used a 470nm light to photoactivate VSCTs bilaterally (from the ventral aspect) in the L1/L2 lumbar segments at P4 using the *ex vivo* spinal cord preparation. As we have shown before (Fig. 4B), photo-activation of VSCTs resulted in robust locomotor-like activity (Fig. 5A).

Bath application of ZD7288 (100μM) abolished locomotor activity during VSCT photoactivation 20 min after exposure (Fig. 5A,B) but in contrast, reduced the locomotor frequency by ~50% after sensory-induced locomotor activity (Fig. 5C,D). However, locomotor behavior was abolished with both induction methods ~40 min after ZD7288 (Fig. 5A–D). These results demonstrate that the I_h current is a major contributor to the production of locomotor behavior during early development and that the channels responsible for the I_h in VSCTs play a prominent role in this behavior.

Since we established that VSCTs are electrically coupled with other VSCTs as well as MNs, we next investigated the impact of electrical coupling in the production of locomotor behavior. The robust locomotor-like activity evoked at P3-P5 by photo-activation of L1/L2 VSCTs expressing ChR2 (after cerebellum injection with CAV2-GFP-CRE in /*s*/-ChR2 mice at P0) was abolished after ~40min of carbenoxolone exposure [gap junction blocker, (Mentis et al., 2005; Tresch and Kiehn, 2000)] (Fig. S5M,N). Photoactivation of VSCTs in the L4/L5 segments also elicited robust locomotor activity that was subsequently abolished after addition of carbenoxolone demonstrating that activation of VSCTs in different lumbar segments also produces locomotor-like activity (Fig. 5E,F).

Lastly, we tested the involvement of electrical coupling following electrically-induced locomotor activity by stimulation of either MN axons (via VRs) or sensory fibers (via DRs) in the same spinal cord *ex vivo* preparations in which VSCTs were photo-activated. MN axon stimulation produced robust locomotor activity, while exposure to 100μM carbenoxolone abolished this activity (Fig. 5G,H). Similarly, DR stimulation resulted in locomotor activity of similar frequency to that produced by VR stimulation. Exposure to carbenoxolone abolished the locomotor behavior (Fig. 5I,J). These results demonstrate that both I_h and electrical coupling contribute to the production of locomotor behavior following activation of VSCTs.

Circuit connectivity between VSCTs, motor neurons and Chx10$^+$ spinal interneurons

To determine how VSCTs coordinate the production of locomotor behavior, we examined the circuit connectivity of VSCTs within the spinal cord by focusing on their outputs. We first sought to identify the neurotransmitter utilized by VSCTs marked by CTb-488 from cerebellum, using fluorescence *in situ* hybridization against the vesicular glutamate transporter 2 (VGluT2). Nearly all VSCTs (~93%, N=3) express VGluT2 (Fig. 6A,B),

similar to DSCTs (~91%, N=3) at P4. This result establishes that VSCTs are excitatory neurons, validating the proposal that SCTs are glutamatergic in nature (Atkinson et al., 2004).

VSCTs in the adult cat possess axon collaterals within the spinal cord (Bras et al., 1988). We used Neurobiotin to reveal the morphology of VSCTs that were intracellularly recorded and subsequently filled and found evidence of spinal axon collaterals in neonatal VSCTs projecting both ipsilaterally and contralaterally to the VSCT soma (Fig. 6C–D and Fig. S6A–C). To investigate the presence of axon collaterals in a larger number of VSCTs, we first injected CTb-647 together with CAV2-Cre virus into the cerebellum of newborn mice and then injected AAV9-CBh-DiO-eGFP (AAV carrying a flexed reporter) directly into the lumbar spinal segments a few days later (~P5-7) to transduce VSCTs and ultimately visualize their axon collaterals (Fig. S6D). The efficiency of the AAV9-CBh-DiO-eGFP to label VSCTs was relatively low, allowing to reveal the full somato-dendritic and axonal trajectory in individual VSCTs (Fig. S6E). We used Neurolucida to reconstruct VSCTs that possess axon collaterals (Fig. S6F–H), and the identity of the axon and its collaterals was verified by Ankyrin G (axonal marker) immunoreactivity in some VSCTs (Fig. S6I,J). We observed axon collaterals in seven VSCTs (53%, 7/13). In six additional VSCTs, we did not observe axon collaterals along the visible length of the main axon, although they may contain axon collaterals at different spinal segments. Overall, these experiments indicate that ~55% of VSCTs possess axon collaterals.

To reveal the territory of synapses from axon collaterals of SCTs, we marked synapses from SCT axon collaterals within the L1/L2 lumbar segments, by colocalization of CTb488 (cerebellum injection at P0), together with Synaptophysin and VGluT2 immunoreactivity at P5 (Fig. S7A–D, N=4) using single plane confocal images and ImageJ analysis (see Methods). These synapses were located medially in the intermediate grey matter and within the MN nucleus, while very few synapses were found in the lateral aspect of the intermediate grey matter or the dorsal horn (Fig. S7D).

We also found that VSCTs directly contact ipsilateral and contralateral MNs (Fig. S7E,F) as well as spinal interneurons since VSCTs' axon collaterals were observed in the intermediate gray matter. To uncover the identity of the spinal interneurons contacted by VSCT axon collaterals, we investigated whether VSCTs synapse with $Chx10^{+}$ spinal neurons. We used a rabies (N2c) virus engineered to cross a single synapse in a retrograde fashion to identify neurons monosynaptically connected to a "starter" population (Reardon et al., 2016), in this case $Chx10^{+}$ neurons. We injected Cre-conditional AAVs into the spinal cord of Chx10-Cre mice to restrict rabies glycoprotein (G) and TVA to $Chx10^{+}$ neurons (Fig. 6E,F). Concurrently, we injected CTb-647 into the cerebellum to label VSCTs. After ~10 days, we injected rabies-N2c-EnvA-dsRed into the spinal lumbar segments. This virus, directly infects only Chx10+ neurons and presynaptic neurons. Accordingly, the $Chx10^{+}$ "starter" population was labeled with a nuclear GFP (nGFP) and dsRed in the cytoplasm, while cells providing monosynaptic input to the starter population were labeled with dsRed only. Morphological analysis revealed one or more VSCTs (CTb^{+} and ventral horn location) that were monosynaptically connected to $Chx10^{+}$ neurons (Fig. 6G,H). These experiments indicated that VSCTs target $Chx10^{+}$ spinal neurons as well as MNs. Importantly, they also

showed morphological evidence of VSCT axon collaterals forming synapses with the soma and dendrites of Chx10^{+} neurons in adult mice (Fig. 6G, arrows).

We next investigated the extent of the VSCT axon collaterals' projection within the spinal cord by injecting two different CTb fluorescent tracers into the cerebellum and the L5/L6 caudal lumbar spinal cord segments at birth (Fig. S7G). At ~P5, we examined the L1/L2 segments for VSCTs that expressed both fluorescent tracers. We found that ~34% of the L1/L2 VSCTs were double-labeled (Fig. S7H,I), demonstrating that VSCTs send descending axon collaterals to caudal spinal segments in addition to their main ascending axon to the cerebellum. Thus, VSCTs form local and extra-segmental spinal circuits with MNs, Chx10^{+} neurons and likely with other spinal neurons via their axon collaterals.

Silencing SCTs in adult mice perturbs locomotor behavior

To investigate whether SCTs are essential for mammalian locomotor behavior in adult mice, we chemogenetically silenced SCTs in freely moving adult (P35-45) mice. We first investigated whether there are any direct connections from the cerebellum to the spinal cord in mice as previously postulated in cats (Matsushita and Hosoya, 1978), rats (Bentivoglio and Kuypers, 1982) and mice (Sathyamurthy et al., 2020), by injecting CTb-555 in the L2/3 spinal cord *in vivo* at P0 or P21 and examined the cerebellum at P4 and P35, respectively. We found no evidence of CTb-555 labelled neurons in the deep cerebellar nuclei either at P4 (Fig. S8A–E) or at P35 (Fig. S8F–J), indicating the lack of direct connections from the cerebellum to the lumbar spinal cord at these ages. To further exclude any potential effects of cerebello-spinal connections that might have been missed by CTb retrograde labelling, we used Cdx2^{FlpO} mice crossed with *fsf-lsl*-h4MDi mice to generate Cdx2^{FlpO}::*fsf-/s/-*h4MDi mice. In this way, we excluded not only any potential direct connections between cerebellum and spinal cord but also any effects of brain neurons possibly transduced from the cerebellum injections, thus limiting the expression of h4MDi to SCTs only, as Cdx2 is solely expressed in spinal cord (Abraira et al., 2017).

CAV2-GFP-CRE or CAV2-GFP or CTb647 (for counting neurons) was injected into the cerebellum of Cdx2^{FlpO}::*fs/-/s/*-h4MDi mice at P21 (Fig. 7A) and experiments performed at P35-45, resulting in ~750 CTb647^{+} VSCTs in the L1 segment (Fig. 7B,C and Methods). We then counted the number of VSCTs in the L1 segment expressing GFP and found that ~400 VSCTs were transduced with CAV2-GFP-CRE (Fig. 7D$_{1\text{-}3}$, E), which corresponds to a ~53% transduction efficiency comparable to that in neonates (Fig. 4N). Expression of DREADDs within VSCTs was confirmed by immunoreactivity against the HA tag co-localizing with CTb-647-labeled spinal neurons from the injected cerebellum (Fig. S9A). Importantly, no HA immunoreactivity was observed in the cerebellum (Fig. S9B), hippocampus (Fig. S9C), cortex (Fig. S9D), and brainstem (Fig. S9E). In addition, selective Cdx2 expression throughout the spinal cord was confirmed by detecting mCherry fluorescence (Fig. S9F). GFP^{+} SCTs were found in the cervical (Fig. S9G), thoracic (Fig. S9H) and caudal lumbar (Fig. S9I) spinal segments. Thus, only SCTs expressed the inhibitory DREADD receptors, ruling out any contributions from the brain during exposure to CNO.

Mice injected at P21 with CAV2-GFP-CRE (or CAV2-GFP) were injected with CNO (5mg/kg, i.p.) at P35-45 to silence SCTs. To assess quantitatively the locomotor ability of freely moving mice, we utilized the open field assay and measured the distance travelled for 10 minutes every hour for a total of six hours. At the onset of the experiment (first 10 minutes following CNO injection) there was no statistical difference between CAV2-GFP-CRE and CAV2-GFP groups (Fig. 7F_1,G). Mice in the CAV2-GFP-CRE group revealed a progressive reduction in the distance travelled at one hour post CNO injection compared to the controls (Fig. 7G). Strikingly, the majority of mice in the CAV2-GFP-CRE group stopped moving between two and three hours post CNO injection (Fig. 7F_2,G and Fig. S9J,K). As expected, the effects of CNO declined four hours after CNO injection and CAV2-GFP-CRE mice started moving around again (Fig. 7G and Fig. S9J,K).

To investigate further the locomotor ability of adult mice in which SCTs were “silenced”, we used a swim test as a proxy for the locomotor CPG. Adult mice (~P35-P45) in which SCTs were chemically “silenced” by exposure to CNO were tested during free swimming. $Cdx2^{FlpO}$::*fsf*-/*s*/-h4MDi injected with either CAV2-GFP or CAV2-CRE were examined just prior to 10mg/kg (equivalent dose to *ex vivo* experiments) CNO injection and 3 hours after CNO injection, which we determined to be the optimal time point for the effect of CNO. High speed videography was used in mice freely swimming for 30 seconds. We found that there was no statistical difference in the ability and total swim period between the two groups before CNO administration (Fig. 7H). In striking contrast, mice that received CAV2-CRE cerebellum injections exhibited a strong reduction in their ability to swim 3 hours after CNO administration [Video #1a (preCNO) and #1b (3h CNO) for mouse A; Video #2a (preCNO) and Video #2b (3h CNO) for Mouse B). These mice exhibited a “floating” behavior during which their overall inability to swim was interspersed with short periods of swimming (Fig. 7H and Videos #1–#2). Control mice were able to swim for the entire testing period after 3h from CNO administration (Fig. 7H and Video #3a (PreCNO) and Video #3b (3h CNO) for mouse C), indicating that CNO itself did not have any effects on swimming behavior. The total period which mice were able to swim was significantly reduced in mice injected with CAV2-CRE (Fig. 7H). Quantification of the maximum hindlimb stroke frequency revealed that mice in the CAV2-CRE group displayed significantly lower maximum frequency compared to controls during the short periods in which they were able to swim (Fig. 7I). Taken together, our experiments demonstrate that mice with “silenced” SCTs have significantly compromised ability to produce locomotor activity during both early postnatal development and in adulthood, pointing to VSCTs as essential drivers of mammalian locomotion.

Discussion

Our discovery that VSCTs are core components of the CPG that are both necessary and sufficient for locomotor behavior represents a paradigm shift in our understanding of the mechanisms of locomotion. Instead of a distributed network responsible for locomotion, the neural control of locomotion may use VSCTs as a nodal point. Sensory inputs and descending supraspinal pathways (Baldissera and Roberts, 1975; Jankowska et al., 2011; Shakya Shrestha et al., 2012; Shrestha et al., 2012) as well as MN input (Falgairolle et al., 2017; Mentis et al., 2005) are all known pathways that initiate or regulate locomotion

and converge on VSCTs. Our findings identify an unexpected function for VSCTs as key controllers of mammalian locomotion and demonstrate that a single neuronal type is essential for such behavior, fundamentally changing the way we think complex behaviors are produced.

Although the initiation of vertebrate locomotion takes place in the brain (Garcia-Rill, 1986; Jordan et al., 2008) and neurons in the brainstem can halt locomotion (Bouvier et al., 2015), the rhythm and pattern generation is solely produced by spinal neurons known as the locomotor CPG (Grillner, 2003; Kiehn, 2006). Several types of excitatory interneurons originating from some progenitor domains (V0, V2, V3) have been proposed as putative rhythm generators (Gosgnach et al., 2017; Kiehn, 2016; Ziskind-Conhaim and Hochman, 2017). However, none of these interneurons is by itself necessary and sufficient for rhythm generation, which has led to the current view that rhythm generation is not mediated by a single, homogenous group of excitatory neurons (Kiehn, 2016).

Our study challenges this hypothesis and proposes that a single neuronal type initiates the locomotor CPG by demonstrating the necessity and sufficient of VSCTs to produce locomotor activity. VSCTs are glutamatergic, project ipsilaterally as well as contralaterally, and possess both intra- and inter-segmental axon collaterals making contacts with MNs, $Chx10^+$ spinal neurons and likely other spinal neurons.

The CPG is active at birth and has been under investigations for decades utilizing the neonatal *ex vivo* spinal cord as an experimental system. By providing exceptional accessibility to the activity and function of CPG neurons, this approach combined with mouse genetics, physiological and anatomical assays has transformed our capabilities to unravel the organization of the locomotor CPG (Jiang et al., 1999; Kiehn, 2016; O'Donovan et al., 2010; Smith and Feldman, 1987; Ziskind-Conhaim et al., 2010). Activation of $VGluT2^+$ neurons was shown to induce locomotor-like activity in neonates (Hagglund et al., 2010). However, $Sim1^+$ (Zhang et al., 2008) and $Chx10^+$ (Crone et al., 2008) neurons, both of which are $VGluT2^+$, were found to play a role in left-right coordination only (Ziskind-Conhaim and Hochman, 2017). In contrast, our findings show that VSCTs are $VGluT2^+$ neurons essential for the induction of locomotor behavior.

Locomotor-like activity can be evoked by sensory stimulation (Bonnot et al., 2002; Lev-Tov et al., 2000), exposure to pharmacological substances (Bonnot et al., 2002; Cazalets et al., 1995; Kjaerulff and Kiehn, 1996), and stimulation of MN axons (Mentis et al., 2005). The latter is considered a puzzling observation, since MNs are thought to act solely as the mediators of central commands to skeletal muscles. However, MNs have recently been proposed to provide feedback to the CPG during locomotor activity (Falgairolle et al., 2017; Song et al., 2016). Together, these observations raised the possibility that MNs may contact a yet unknown interneuron that is key for the locomotor CPG. However, silencing of Renshaw cells and $Sim1^+$ interneurons, which are the only spinal interneurons contacted by MN axon collaterals known to date, did not affect locomotor rhythmogenesis (Enjin et al., 2017; Zhang et al., 2008). Our identification of VSCTs as a target of MN axon collaterals provides an answer to this conundrum. VSCTs receive monosynaptic activation from MNs that is both cholinergic and glutamatergic in nature, consistent with previous findings that

spinal MNs axon collaterals release both acetylcholine and glutamate or aspartate (Mentis et al., 2005; Nishimaru et al., 2005; Richards et al., 2014). These observations point to a positive feedback neuronal circuit between MNs and VSCTs that enables early, robust activation of VSCTs and subsequent activation of other neurons involved in locomotor behavior.

We also discovered that VSCTs are electrically coupled amongst themselves. What is the importance of this electrical coupling in the context of locomotor rhythmogenesis? In the developing mammalian spinal cord, locomotor-like rhythm generation can be produced solely through gap junctions (Tresch and Kiehn, 2000). We propose that gap junctions amongst VSCTs are critical for the induction of locomotor rhythmogenesis. Accordingly, we reveal that gap junction blockade using carbenoxolone abolishes locomotor behavior induced in neonates by i) direct photoactivation of VSCTs, ii) sensory stimulation, or iii) MN axon stimulation. Electrical communication amongst spinal neurons is thought to be an important circuit mechanism in the locomotor CPG (Ziskind-Conhaim and Hochman, 2017), and we argue that a key function of electrical coupling amongst VSCTs is to synchronize their activity. In addition, chemical neurotransmission may not be necessary for the production of rhythmic output across the rostro-caudal axis since photoactivation of VSCTs in either the rostral (L1/L2) or the caudal (L4/L5) spinal segments resulted in robust locomotor activity.

Intriguingly, some VSCTs also communicate electrically with MNs via gap junctions. Neonatal mammalian MNs are electrically coupled amongst themselves only during the first two postnatal weeks (Chang et al., 1999; Mentis et al., 2002; Personius et al., 2007; Walton and Navarrete, 1991). Our findings that VSCTs are electrically coupled with a subset of MNs indicate that electrical coupling is not selective amongst a single neuronal type. Moreover, an important implication of these findings is that depending on the extent and strength of coupling, the phase change in their respective membrane potential during the locomotor behavior will be similar and likely contribute to the recruitment of VSCTs as well as the neuronal targets of their axon collaterals.

The observation that VSCTs possess rhythmogenic properties provides additional mechanistic support to their function as essential neurons for locomotor rhythmogenesis. VSCTs possess the I_h current that has been previously implicated as a key cellular property in rhythmic behaviors such as in the inspiratory pre-Bötzinger complex neurons in mice (Thoby-Brisson et al., 2000) or in the rhythmic behavior of pyloric neurons of the stomato-gastric ganglion in lobsters (Zhang et al., 2003). I_h is strongly activated by hyperpolarization (Pape, 1996) as well as in a time- and voltage-dependent membrane conductance. While the precise role of I_h in VSCTs during locomotor activity remains to be elucidated, it is possible that I_h may limit the effect of rhythmic inhibition and cause the membrane potential to escape more rapidly from inhibition during locomotor activity. In addition, since I_h regulates the post-inhibitory rebound potential and neuronal excitability, I_h may also be involved in the acceleration of the arrival of the first AP and thus contribute to the enhanced recruitment of VSCTs. Finally, in tadpoles I_h has been shown to mask an ultraslow AHP generated by sodium-potassium pumps that would normally inhibit activity (Picton et al., 2018), so the presence of I_h may also influence the excitability state of VSCTs.

VSCTs were first discovered by Sherrington (Cooper and Sherrington, 1940) and have been hypothesized to serve as “efferent copies” of spinal motor networks (Lundberg, 1971), whereby they provide the cerebellum with feedback information regarding the ongoing state of the ventral spinal cord. During repetitive motor tasks, like locomotion or scratching, signals from the spinal CPG evoke rhythmic activity in the cerebellar cortex whose outputs modulate the descending tracts that regulate the spinal rhythmic activity (Grillner and Wallén, 1985; Martínez-Silva et al., 2014; Morton and Bastian, 2003; Rand et al., 1998). The cerebellum-brainstem-spinal cord loop is essential for coordinated and adaptive gait control. However, the cerebellum is not critical to generate locomotion, rather it modulates limb movement patterns, balance and adaptation (Hammar et al., 2011; Pisotta and Molinari, 2014). Our findings that VSCTs are essential for the initiation and maintenance of locomotion imply that VSCTs are not purely a relay messenger of information as originally proposed. Instead, in addition to their role in coordinating locomotion at the spinal level, VSCT output to the cerebellum may be critical for the regulation of locomotion by the cerebellum and other supraspinal areas influenced by cerebellar output. To this end, and although the precise neuronal circuit mechanisms involving VSCTs in adult locomotion remain to be elucidated, our observations that $Chx10^+$ spinal neurons are synaptic targets of VSCT axon collaterals in adults provides a potential insight. $Chx10^+$ spinal neurons are known to be activated during adult locomotion (Al-Mosawie et al., 2007), and have been shown to function in the maintenance of locomotor rhythmicity and in left-right alternation (Crone et al., 2008; Crone et al., 2009). Thus, we suggest that $Chx10^+$ spinal neurons receive significant activation by VSCTs during adult locomotion and without which the animal’s locomotor ability is significantly compromised. The importance of the spinal axon collaterals of VSCTs versus their main ascending axon to the cerebellum for the induction of locomotor behavior is underscored by observations in which *in vivo* adult spinalized mice were able to produce fictive locomotion (Meehan et al., 2012; Meehan et al., 2017). In addition, cerebellectomy has been shown to have little impact on the ability of other organisms to locomote, including fish (Roberts et al., 1992), rats (Federico et al., 2006), cats (Udo et al., 1980), monkeys (Wirth and O’Leary, 1974) as well as in humans either due to cerebellum agenesis or cerebellar resection due to tumors (Earhart and Bastian, 2001; Ilg et al., 2008; Yu et al., 2015).

In conclusion, we discovered that VSCTs are both necessary and sufficient for locomotor behavior and that they are core components of the locomotor CPG. It provides also the conceptual foundation for developing therapeutic approaches for patients suffering from spinal cord injury and motor disorders.

Limitations of the Study

One limitation of our study is that we cannot fully exclude the potential involvement of DSCTs in locomotor behavior in adult mice as we demonstrated in neonatal mice. The optogenetic approaches used in neonates cannot be employed in adult mice for technical reasons. However, DSCTs, including Clarke’s column neurons, do not possess axon collaterals in the cat (Edgley and Gallimore, 1988; Houchin et al., 1983), whereas VSCTs possess spinal axon collaterals both in cats (Bras et al., 1988) and in mice (this study). If DSCTs indeed lack spinal axon collaterals as is the case in cat, it is conceivable

that DSCTs do not have access to spinal locomotor circuits and therefore might not be involved in locomotor rhythmogenesis. To further dissect the direct role of these two SCTs, future experiments are needed in which yet-to-be identified genetic markers that selectively label DSCTs and VSCTs could be used to either activate or silence them selectively using Cre-Lox recombination and floxed chemogenetic approaches.

Supplementary Material

Refer to Web version on PubMed Central for supplementary material.

Acknowledgements:

We thank D. Ginty for the Cdx2^{FlpO} mice and T. Jessell for the Chx10^{Cre} mice. We are also grateful to L. Pellizzoni, S. Przedborski, F.J. Alvarez, J. Gogos and M.J. O'Donovan and members of the Mentis lab for comments on the manuscript. G.Z.M. is supported by NINDS, NIH (R01-NS078375, R21-NS079981), The NIH Blueprint for Neuroscience Research (R01-AA027079), The SMA Foundation, and Project-ALS. JIC was supported by NINDS, NIH (F30NS098551).

References:

Abraira VE, Kuehn ED, Chirila AM, Springel MW, Toliver AA, Zimmerman AL, Orefice LL, Boyle KA, Bai L, Song BJ, et al. (2017). The Cellular and Synaptic Architecture of the Mechanosensory Dorsal Horn. Cell 168, 295–310.e219. [PubMed: 28041852]

Al-Mosawie A, Wilson JM, and Brownstone RM (2007). Heterogeneity of V2-derived interneurons in the adult mouse spinal cord. The European journal of neuroscience 26, 3003–3015. [PubMed: 18028108]

Alvarez FJ, and Fyffe RE (2007). The continuing case for the Renshaw cell. The Journal of physiology 584, 31–45. [PubMed: 17640932]

Arshavsky YI, Berkinblit MB, Fukson OI, Gelfand IM, and Orlovsky GN (1972). Origin of modulation in neurones of the ventral spinocerebellar tract during locomotion. Brain research 43, 276–279. [PubMed: 5050196]

Atkinson L, Batten TF, Moores TS, Varoqui H, Erickson JD, and Deuchars J (2004). Differential co-localisation of the P2X7 receptor subunit with vesicular glutamate transporters VGLUT1 and VGLUT2 in rat CNS. Neuroscience 123, 761–768. [PubMed: 14706788]

Baldissera F, and Roberts WJ (1975). Effects on the ventral spinocerebellar tract neurones from Deiters' nucleus and the medial longitudinal fascicle in the cat. Acta Physiol Scand 93, 228–249. [PubMed: 167549]

Bentivoglio M, and Kuypers HG (1982). Divergent axon collaterals from rat cerebellar nuclei to diencephalon, mesencephalon, medulla oblongata and cervical cord. A fluorescent double retrograde labeling study. Experimental brain research 46, 339–356. [PubMed: 7095042]

Bonnot A, Mentis GZ, Skoch J, and O'Donovan MJ (2005). Electroporation loading of calcium-sensitive dyes into the CNS. Journal of neurophysiology 93, 1793–1808. [PubMed: 15509647]

Bonnot A, Whelan PJ, Mentis GZ, and O'Donovan MJ (2002). Locomotor-like activity generated by the neonatal mouse spinal cord. Brain research Brain research reviews 40, 141–151. [PubMed: 12589913]

Bouvier J, Caggiano V, Leiras R, Caldeira V, Bellardita C, Balueva K, Fuchs A, and Kiehn O (2015). Descending Command Neurons in the Brainstem that Halt Locomotion. Cell 163, 1191–1203. [PubMed: 26590422]

Bras H, Cavallari P, and Jankowska E (1988). Demonstration of initial axon collaterals of cells of origin of the ventral spinocerebellar tract in the cat. The Journal of comparative neurology 273, 584–592. [PubMed: 2463285]

Britz O, Zhang J, Grossmann KS, Dyck J, Kim JC, Dymecki S, Gosgnach S, and Goulding M (2015). A genetically defined asymmetry underlies the inhibitory control of flexor-extensor locomotor movements. eLife 4.

Cazalets JR, Borde M, and Clarac F (1995). Localization and organization of the central pattern generator for hindlimb locomotion in newborn rat. The Journal of neuroscience : the official journal of the Society for Neuroscience 15, 4943–4951. [PubMed: 7623124]

Chang Q, Gonzalez M, Pinter MJ, and Balice-Gordon RJ (1999). Gap junctional coupling and patterns of connexin expression among neonatal rat lumbar spinal motor neurons. The Journal of neuroscience : the official journal of the Society for Neuroscience 19, 10813–10828. [PubMed: 10594064]

Chen AI, de Nooij JC, and Jessell TM (2006). Graded activity of transcription factor Runx3 specifies the laminar termination pattern of sensory axons in the developing spinal cord. Neuron 49, 395–408. [PubMed: 16446143]

Chopek JW, Nascimento F, Beato M, Brownstone RM, and Zhang Y (2018). Sub-populations of Spinal V3 Interneurons Form Focal Modules of Layered Pre-motor Microcircuits. Cell reports 25, 146–156.e143. [PubMed: 30282024]

Cooper S, and Sherrington CS (1940). Gowers Tract and Spinal Border Cells. Brain 63, 123–134.

Crone SA, Quinlan KA, Zagoraiou L, Droho S, Restrepo CE, Lundfald L, Endo T, Setlak J, Jessell TM, Kiehn O, et al. (2008). Genetic ablation of V2a ipsilateral interneurons disrupts left-right locomotor coordination in mammalian spinal cord. Neuron 60, 70–83. [PubMed: 18940589]

Crone SA, Zhong G, Harris-Warrick R, and Sharma K (2009). In mice lacking V2a interneurons, gait depends on speed of locomotion. The Journal of neuroscience : the official journal of the Society for Neuroscience 29, 7098–7109. [PubMed: 19474336]

Earhart GM, and Bastian AJ (2001). Selection and coordination of human locomotor forms following cerebellar damage. Journal of neurophysiology 85, 759–769. [PubMed: 11160510]

Eccles JC, Fatt P, and Koketsu K (1954). Cholinergic and inhibitory synapses in a pathway from motor-axon collaterals to motoneurones. The Journal of physiology 126, 524–562. [PubMed: 13222354]

Edgley SA, and Gallimore CM (1988). The morphology and projections of dorsal horn spinocerebellar tract neurones in the cat. The Journal of physiology 397, 99–111. [PubMed: 3411522]

Enjin A, Perry S, Hilscher MM, Nagaraja C, Larhammar M, Gezelius H, Eriksson A, Leao KE, and Kullander K (2017). Developmental Disruption of Recurrent Inhibitory Feedback Results in Compensatory Adaptation in the Renshaw Cell-Motor Neuron Circuit. The Journal of neuroscience : the official journal of the Society for Neuroscience 37, 5634–5647. [PubMed: 28483975]

Falgairolle M, Puhl JG, Pujala A, Liu W, and O'Donovan MJ (2017). Motoneurons regulate the central pattern generator during drug-induced locomotor-like activity in the neonatal mouse. eLife 6.

Federico F, Leggio MG, Mandolesi L, and Petrosini L (2006). The NMDA receptor antagonist CGS 19755 disrupts recovery following cerebellar lesions. Restorative neurology and neuroscience 24, 1–7. [PubMed: 16518022]

Fletcher EV, Simon CM, Pagiazitis JG, Chalif JI, Vukojicic A, Drobac E, Wang X, and Mentis GZ (2017). Reduced sensory synaptic excitation impairs motor neuron function via Kv2.1 in spinal muscular atrophy. Nature neuroscience 20, 905–916. [PubMed: 28504671]

Garcia-Rill E (1986). The basal ganglia and the locomotor regions. Brain research 396, 47–63. [PubMed: 2871904]

Gosgnach S, Bikoff JB, Dougherty KJ, El Manira A, Lanuza GM, and Zhang Y (2017). Delineating the Diversity of Spinal Interneurons in Locomotor Circuits. The Journal of neuroscience : the official journal of the Society for Neuroscience 37, 10835–10841. [PubMed: 29118212]

Gosgnach S, Lanuza GM, Butt SJ, Saueressig H, Zhang Y, Velasquez T, Riethmacher D, Callaway EM, Kiehn O, and Goulding M (2006). V1 spinal neurons regulate the speed of vertebrate locomotor outputs. Nature 440, 215–219. [PubMed: 16525473]

Goulding M, and Pfaff SL (2005). Development of circuits that generate simple rhythmic behaviors in vertebrates. Current opinion in neurobiology 15, 14–20. [PubMed: 15721739]

Graham Brown T (1911). The intrinsic factors in the act of progression in the mammal. Proc R Soc Lond B Biol Sci 84, 308–319.

Grillner S (2003). The motor infrastructure: from ion channels to neuronal networks. Nature reviews Neuroscience 4, 573–586. [PubMed: 12838332]

Grillner S, and Wallén P (1985). Central pattern generators for locomotion, with special reference to vertebrates. Annual review of neuroscience 8, 233–261.

Guertin PA (2012). Central pattern generator for locomotion: anatomical, physiological, and pathophysiological considerations. Frontiers in neurology 3, 183. [PubMed: 23403923]

Hagglund M, Borgius L, Dougherty KJ, and Kiehn O (2010). Activation of groups of excitatory neurons in the mammalian spinal cord or hindbrain evokes locomotion. Nature neuroscience 13, 246–252. [PubMed: 20081850]

Hammar I, Krutki P, Drzymala-Celichowska H, Nilsson E, and Jankowska E (2011). A trans-spinal loop between neurones in the reticular formation and in the cerebellum. The Journal of physiology 589, 653–665. [PubMed: 21149461]

Houchin J, Maxwell DJ, Fyffe RE, and Brown AG (1983). Light and electron microscopy of dorsal spinocerebellar tract neurones in the cat: an intracellular horseradish peroxidase study. Quarterly journal of experimental physiology (Cambridge, England) 68, 719–732.

Ilg W, Giese MA, Gizewski ER, Schoch B, and Timmann D (2008). The influence of focal cerebellar lesions on the control and adaptation of gait. Brain : a journal of neurology 131, 2913–2927. [PubMed: 18835866]

Jankowska E, Nilsson E, and Hammar I (2011). Processing information related to centrally initiated locomotor and voluntary movements by feline spinocerebellar neurones. The Journal of physiology 589, 5709–5725. [PubMed: 21930605]

Jiang Z, Carlin KP, and Brownstone RM (1999). An in vitro functionally mature mouse spinal cord preparation for the study of spinal motor networks. Brain research 816, 493–499. [PubMed: 9878874]

Jordan LM, Liu J, Hedlund PB, Akay T, and Pearson KG (2008). Descending command systems for the initiation of locomotion in mammals. Brain research reviews 57, 183–191. [PubMed: 17928060]

Kase D, and Imoto K (2012). The Role of HCN Channels on Membrane Excitability in the Nervous System. Journal of signal transduction 2012, 619747. [PubMed: 22934165]

Kiehn O (2006). Locomotor circuits in the mammalian spinal cord. Annual review of neuroscience 29, 279–306.

Kiehn O (2016). Decoding the organization of spinal circuits that control locomotion. Nature reviews Neuroscience 17, 224–238. [PubMed: 26935168]

Kiehn O, and Butt SJ (2003). Physiological, anatomical and genetic identification of CPG neurons in the developing mammalian spinal cord. Progress in neurobiology 70, 347–361. [PubMed: 12963092]

Kjaerulff O, and Kiehn O (1996). Distribution of networks generating and coordinating locomotor activity in the neonatal rat spinal cord in vitro: a lesion study. The Journal of neuroscience : the official journal of the Society for Neuroscience 16, 5777–5794. [PubMed: 8795632]

Lev-Tov A, Delvolvé I, and Kremer E (2000). Sacrocaudal afferents induce rhythmic efferent bursting in isolated spinal cords of neonatal rats. Journal of neurophysiology 83, 888–894. [PubMed: 10669502]

Lundberg A (1971). Function of the ventral spinocerebellar tract. A new hypothesis. Experimental brain research 12, 317–330. [PubMed: 5553376]

Lüthi A, and McCormick DA (1998). H-current: properties of a neuronal and network pacemaker. Neuron 21, 9–12. [PubMed: 9697847]

Manvich DF, Webster KA, Foster SL, Farrell MS, Ritchie JC, Porter JH, and Weinshenker D (2018). The DREADD agonist clozapine N-oxide (CNO) is reverse-metabolized to clozapine and produces clozapine-like interoceptive stimulus effects in rats and mice. Scientific reports 8, 3840. [PubMed: 29497149]

Martínez-Silva L, Manjarrez E, Gutiérrez-Ospina G, and Quevedo JN (2014). Electrophysiological representation of scratching CpG activity in the cerebellum. PloS one 9, e109936. [PubMed: 25350378]

Matsushita M, and Hosoya Y (1978). The location of spinal projection neurons in the cerebellar nuclei (cerebellospinal tract neurons) of the cat. A study with the horseradish peroxidase technique. Brain research 142, 237–248. [PubMed: 630384]

Meehan CF, Grondahl L, Nielsen JB, and Hultborn H (2012). Fictive locomotion in the adult decerebrate and spinal mouse in vivo. The Journal of physiology 590, 289–300. [PubMed: 22106172]

Meehan CF, Mayr KA, Manuel M, Nakanishi ST, and Whelan PJ (2017). Decerebrate mouse model for studies of the spinal cord circuits. Nature protocols 12, 732–747. [PubMed: 28277546]

Mendelsohn AI, Simon CM, Abbott LF, Mentis GZ, and Jessell TM (2015). Activity Regulates the Incidence of Heteronymous Sensory-Motor Connections. Neuron 87, 111–123. [PubMed: 26094608]

Mentis GZ, Alvarez FJ, Bonnot A, Richards DS, Gonzalez-Forero D, Zerda R, and O'Donovan MJ (2005). Noncholinergic excitatory actions of motoneurons in the neonatal mammalian spinal cord. Proceedings of the National Academy of Sciences of the United States of America 102, 7344–7349. [PubMed: 15883359]

Mentis GZ, Blivis D, Liu W, Drobac E, Crowder ME, Kong L, Alvarez FJ, Sumner CJ, and O'Donovan MJ (2011). Early functional impairment of sensory-motor connectivity in a mouse model of spinal muscular atrophy. Neuron 69, 453–467. [PubMed: 21315257]

Mentis GZ, Díaz E, Moran LB, and Navarrete R (2002). Increased incidence of gap junctional coupling between spinal motoneurones following transient blockade of NMDA receptors in neonatal rats. The Journal of physiology 544, 757–764. [PubMed: 12411521]

Mentis GZ, Siembab VC, Zerda R, O'Donovan MJ, and Alvarez FJ (2006). Primary afferent synapses on developing and adult Renshaw cells. The Journal of neuroscience : the official journal of the Society for Neuroscience 26, 13297–13310. [PubMed: 17182780]

Morton SM, and Bastian AJ (2003). Relative contributions of balance and voluntary leg-coordination deficits to cerebellar gait ataxia. Journal of neurophysiology 89, 1844–1856. [PubMed: 12612041]

Nishimaru H, Restrepo CE, Ryge J, Yanagawa Y, and Kiehn O (2005). Mammalian motor neurons corelease glutamate and acetylcholine at central synapses. Proceedings of the National Academy of Sciences of the United States of America 102, 5245–5249. [PubMed: 15781854]

Noga BR, Shefchyk SJ, Jamal J, and Jordan LM (1987). The role of Renshaw cells in locomotion: antagonism of their excitation from motor axon collaterals with intravenous mecamylamine. Experimental brain research 66, 99–105. [PubMed: 3582539]

O'Donovan MJ, Bonnot A, Mentis GZ, Chub N, Pujala A, and Alvarez FJ (2010). Mechanisms of excitation of spinal networks by stimulation of the ventral roots. Annals of the New York Academy of Sciences 1198, 63–71. [PubMed: 20536921]

Pape HC (1996). Queer current and pacemaker: the hyperpolarization-activated cation current in neurons. Annual review of physiology 58, 299–327.

Pastor AM, Mentis GZ, De La Cruz RR, Díaz E, and Navarrete R (2003). Increased electrotonic coupling in spinal motoneurons after transient botulinum neurotoxin paralysis in the neonatal rat. Journal of neurophysiology 89, 793–805. [PubMed: 12574457]

Personius KE, Chang Q, Mentis GZ, O'Donovan MJ, and Balice-Gordon RJ (2007). Reduced gap junctional coupling leads to uncorrelated motor neuron firing and precocious neuromuscular synapse elimination. Proceedings of the National Academy of Sciences of the United States of America 104, 11808–11813. [PubMed: 17609378]

Picton LD, Sillar KT, and Zhang HY (2018). Control of Xenopus Tadpole Locomotion via Selective Expression of Ih in Excitatory Interneurons. Current biology : CB 28, 3911–3923.e3912. [PubMed: 30503615]

Pisotta I, and Molinari M (2014). Cerebellar contribution to feedforward control of locomotion. Frontiers in human neuroscience 8, 475. [PubMed: 25009490]

Rand MK, Wunderlich DA, Martin PE, Stelmach GE, and Bloedel JR (1998). Adaptive changes in responses to repeated locomotor perturbations in cerebellar patients. Experimental brain research 122, 31–43. [PubMed: 9772109]

Reardon TR, Murray AJ, Turi GF, Wirblich C, Croce KR, Schnell MJ, Jessell TM, and Losonczy A (2016). Rabies Virus CVS-N2c(ΔG) Strain Enhances Retrograde Synaptic Transfer and Neuronal Viability. Neuron 89, 711–724. [PubMed: 26804990]

Renshaw B (1946). Central effects of centripetal impulses in axons of spinal ventral roots. Journal of neurophysiology 9, 191–204. [PubMed: 21028162]

Richards DS, Griffith RW, Romer SH, and Alvarez FJ (2014). Motor axon synapses on renshaw cells contain higher levels of aspartate than glutamate. PloS one 9, e97240. [PubMed: 24816812]

Roberts BL, van Rossem A, and de Jager S (1992). The influence of cerebellar lesions on the swimming performance of the trout. The Journal of experimental biology 167, 171–178. [PubMed: 1634862]

Rothberg BS, Shin KS, Phale PS, and Yellen G (2002). Voltage-controlled gating at the intracellular entrance to a hyperpolarization-activated cation channel. The Journal of general physiology 119, 83–91. [PubMed: 11773240]

Sathyamurthy A, Barik A, Dobrott CI, Matson KJE, Stoica S, Pursley R, Chesler AT, and Levine AJ (2020). Cerebellospinal Neurons Regulate Motor Performance and Motor Learning. Cell reports 31, 107595. [PubMed: 32402292]

Shakya Shrestha S, Bannatyne BA, Jankowska E, Hammar I, Nilsson E, and Maxwell DJ (2012). Inhibitory inputs to four types of spinocerebellar tract neurons in the cat spinal cord. Neuroscience 226, 253–269. [PubMed: 22989920]

Shrestha SS, Bannatyne BA, Jankowska E, Hammar I, Nilsson E, and Maxwell DJ (2012). Excitatory inputs to four types of spinocerebellar tract neurons in the cat and the rat thoraco-lumbar spinal cord. J Physiol 590, 1737–1755. [PubMed: 22371473]

Simon CM, Dai Y, Van Alstyne M, Koutsioumpa C, Pagiazitis JG, Chalif JI, Wang X, Rabinowitz JE, Henderson CE, Pellizzoni L, et al. (2017). Converging Mechanisms of p53 Activation Drive Motor Neuron Degeneration in Spinal Muscular Atrophy. Cell reports 21, 3767–3780. [PubMed: 29281826]

Smith JC, and Feldman JL (1987). In vitro brainstem-spinal cord preparations for study of motor systems for mammalian respiration and locomotion. Journal of neuroscience methods 21, 321–333. [PubMed: 2890797]

Song J, Ampatzis K, Björnfors ER, and El Manira A (2016). Motor neurons control locomotor circuit function retrogradely via gap junctions. Nature 529, 399–402. [PubMed: 26760208]

Talpalar AE, Bouvier J, Borgius L, Fortin G, Pierani A, and Kiehn O (2013). Dual-mode operation of neuronal networks involved in left-right alternation. Nature 500, 85–88. [PubMed: 23812590]

Thoby-Brisson M, Telgkamp P, and Ramirez JM (2000). The role of the hyperpolarization-activated current in modulating rhythmic activity in the isolated respiratory network of mice. The Journal of neuroscience : the official journal of the Society for Neuroscience 20, 2994–3005. [PubMed: 10751452]

Tresch MC, and Kiehn O (2000). Motor coordination without action potentials in the mammalian spinal cord. Nature neuroscience 3, 593–599. [PubMed: 10816316]

Udo M, Matsukawa K, Kamei H, and Oda Y (1980). Cerebellar control of locomotion: effects of cooling cerebellar intermediate cortex in high decerebrate and awake walking cats. Journal of neurophysiology 44, 119–134. [PubMed: 7420131]

Walton KD, and Navarrete R (1991). Postnatal changes in motoneurone electrotonic coupling studied in the in vitro rat lumbar spinal cord. The Journal of physiology 433, 283–305. [PubMed: 1668753]

Whelan P, Bonnot A, and O'Donovan MJ (2000). Properties of rhythmic activity generated by the isolated spinal cord of the neonatal mouse. Journal of neurophysiology 84, 2821–2833. [PubMed: 11110812]

Wirth FP, and O'Leary JL (1974). Locomotor behavior of decerebellated arboreal mammals--monkey and raccoon. The Journal of comparative neurology 157, 53–85. [PubMed: 4212146]

Yu F, Jiang QJ, Sun XY, and Zhang RW (2015). A new case of complete primary cerebellar agenesis: clinical and imaging findings in a living patient. Brain : a journal of neurology 138, e353. [PubMed: 25149410]

Zhang J, Lanuza GM, Britz O, Wang Z, Siembab VC, Zhang Y, Velasquez T, Alvarez FJ, Frank E, and Goulding M (2014). V1 and v2b interneurons secure the alternating flexor-extensor motor activity mice require for limbed locomotion. Neuron 82, 138–150. [PubMed: 24698273]

Zhang Y, Narayan S, Geiman E, Lanuza GM, Velasquez T, Shanks B, Akay T, Dyck J, Pearson K, Gosgnach S, et al. (2008). V3 spinal neurons establish a robust and balanced locomotor rhythm during walking. Neuron 60, 84–96. [PubMed: 18940590]

Zhang Y, Oliva R, Gisselmann G, Hatt H, Guckenheimer J, and Harris-Warrick RM (2003). Overexpression of a hyperpolarization-activated cation current (Ih) channel gene modifies the firing activity of identified motor neurons in a small neural network. The Journal of neuroscience : the official journal of the Society for Neuroscience 23, 9059–9067. [PubMed: 14534239]

Ziskind-Conhaim L, and Hochman S (2017). Diversity of molecularly defined spinal interneurons engaged in mammalian locomotor pattern generation. Journal of neurophysiology 118, 2956–2974. [PubMed: 28855288]

Ziskind-Conhaim L, Mentis GZ, Wiesner EP, and Titus DJ (2010). Synaptic integration of rhythmogenic neurons in the locomotor circuitry: the case of Hb9 interneurons. Annals of the New York Academy of Sciences 1198, 72–84. [PubMed: 20536922]

Highlights

- VSCTs have rhythmogenic properties, form circuits with motor neurons and $Chx10^{+}$ neurons
- VSCTs can be activated monosynaptically and electrically by motor neurons
- Activation of VSCTs is sufficient to initiate locomotion during early development
- Silencing VSCTs abolishes locomotor behavior in neonates and perturbs it in adulthood

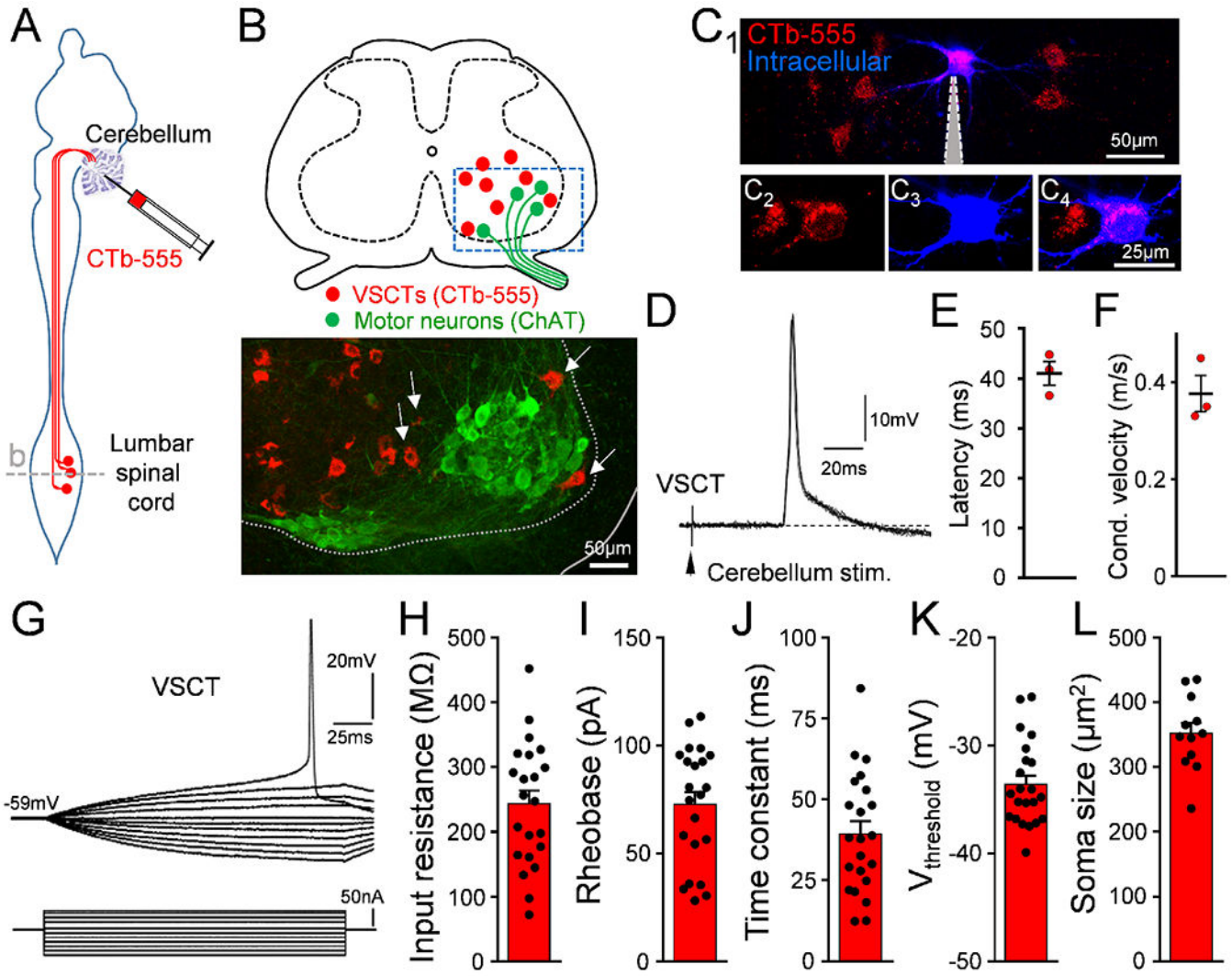

Figure 1. VSCTs located near or within the motor neuron nucleus are hyperexcitable.

(**A**) CTb-555 injected in cerebellum at P0 to label VSCTs in the L1/L2 lumbar spinal cord. (**B**) Drawing of the L2 spinal cord [dashed line in (**A**)] and confocal image from the ventral horn (box in drawing) showing VSCTs (red) near or within (arrows) MNs at P4 (ChAT; green) (N=12). (**C_{1-4}**) Individual VSCTs (CTb-555; red) were visually targeted for intracellular recording (n=22; N=22 mice) using 2P-laser microscopy in the intact *ex vivo* spinal cord (intracellular dye: Cascade Blue dextran). Grey: patch electrode. (**D**) Five superimposed antidromic action potentials (APs) in a P3 L1 VSCT after cerebellum electrical stimulation at 1 Hz. (**E**) Latency of antidromic APs for 3 VSCTs (N=3). (**F**) Conduction velocity. (**G**) Superimposed traces from a current/voltage plot in a P4 L2 VSCT. VSCTs' input resistance (**H**) (n=22), rheobase (**I**), time constant (**J**), threshold for induction of AP (**K**), and soma size (**L**) (n=12). Data are represented as mean ± SEM. See also Fig. S1.

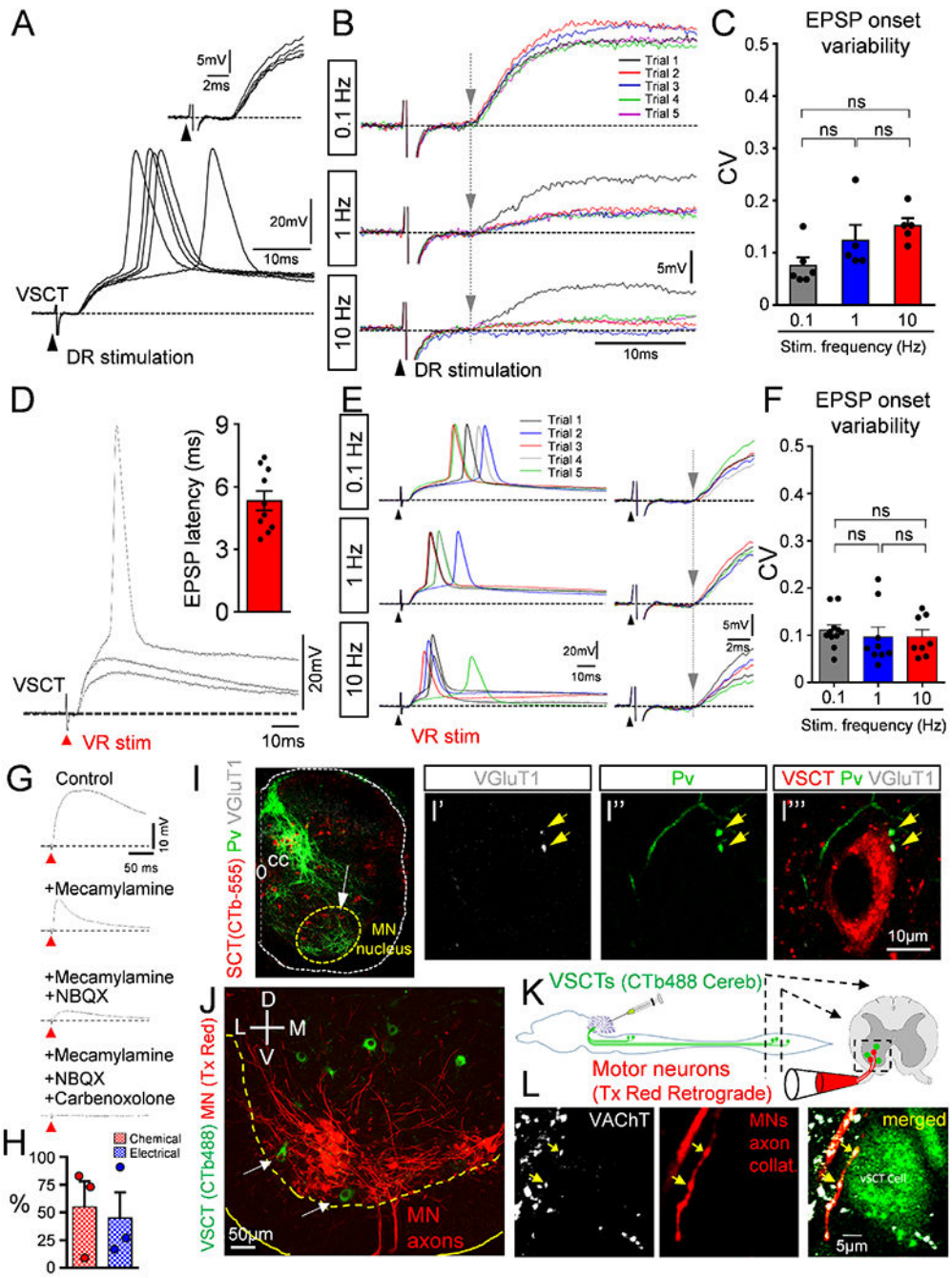

Figure 2. VSCTs receive synapses from proprioceptors and motor neuron axon collaterals

(**A**) Superimposed responses from a P5 L1 VSCT after ipsilateral L1 dorsal root (DR) stimulation. Inset shows constant short latency responses. (**B**) As in (**A**) from a P3 L2 VSCT after ipsilateral DR-L2 stimulation at 0.1, 1 and 10Hz. Consecutive responses are color coded. Grey vertical line indicates constant latency of the response onset. (**C**) Coefficient of variation (CV) of latency in the onset of EPSP in VSCTs after DR stimulation (ns: no significance; One Way ANOVA, Brown-Forsythe test). (**D**) Superimposed graded EPSPs from a P4 L2 VSCT after ipsilateral homosegmental ventral root (VR) stimulation. Inset:

latency of EPSPs in 10 VSCTs. (**E**) As in (**D**) from a P4 L2 VSCT after ipsilateral VR-L2 stimulation at 0.1, 1 and 10Hz. Traces on the right are expanded in time. Grey vertical line indicates constant latency. (**F**) CV of the onset of EPSPs in VSCTs evoked by VR stimulation (One Way ANOVA). (**G**) EPSP in a P4 L2 VSCT after ipsilateral VR stimulation in control solution, and sequential addition of mecamylamine (50μM), NBQX (20μM) and carbenoxolone (100μM). (**H**) Percentage of response in VSCTs due to chemical (red) and electrical (blue) transmission (n=3 VSCTs, N=3 mice). (**I**) SCTs (CTb-555; red), parvalbumin (green) and VGlu1 (white) immunoreactivity in L1 at P4 (n=7). (**I**’-**I**’”) L1 proprioceptive fibers (parvalbumin; green) and $VGluT1^{+}$ synapses (white; yellow arrows) onto a VSCT (red) shown by white arrow in (**I**). (**J**) Ventral horn confocal image showing VSCTs (green) located close or within (arrows) the MN (red) nucleus. (**K**) Protocol in which CTb-488 injected in cerebellum at P0 to label VSCTs (green). At P4, MNs were backfilled with Texas Red dextran (red) from the VR using *ex vivo* spinal cord. (**L**) Single plane confocal images showing VAChT immunoreactivity (white), MN axon collaterals (red) and a VSCT (green), revealing two synapses (yellow arrows) (n=7 VSCTs, N=3 mice). Data are represented as mean ± SEM. See also Figs. S1 and S2.

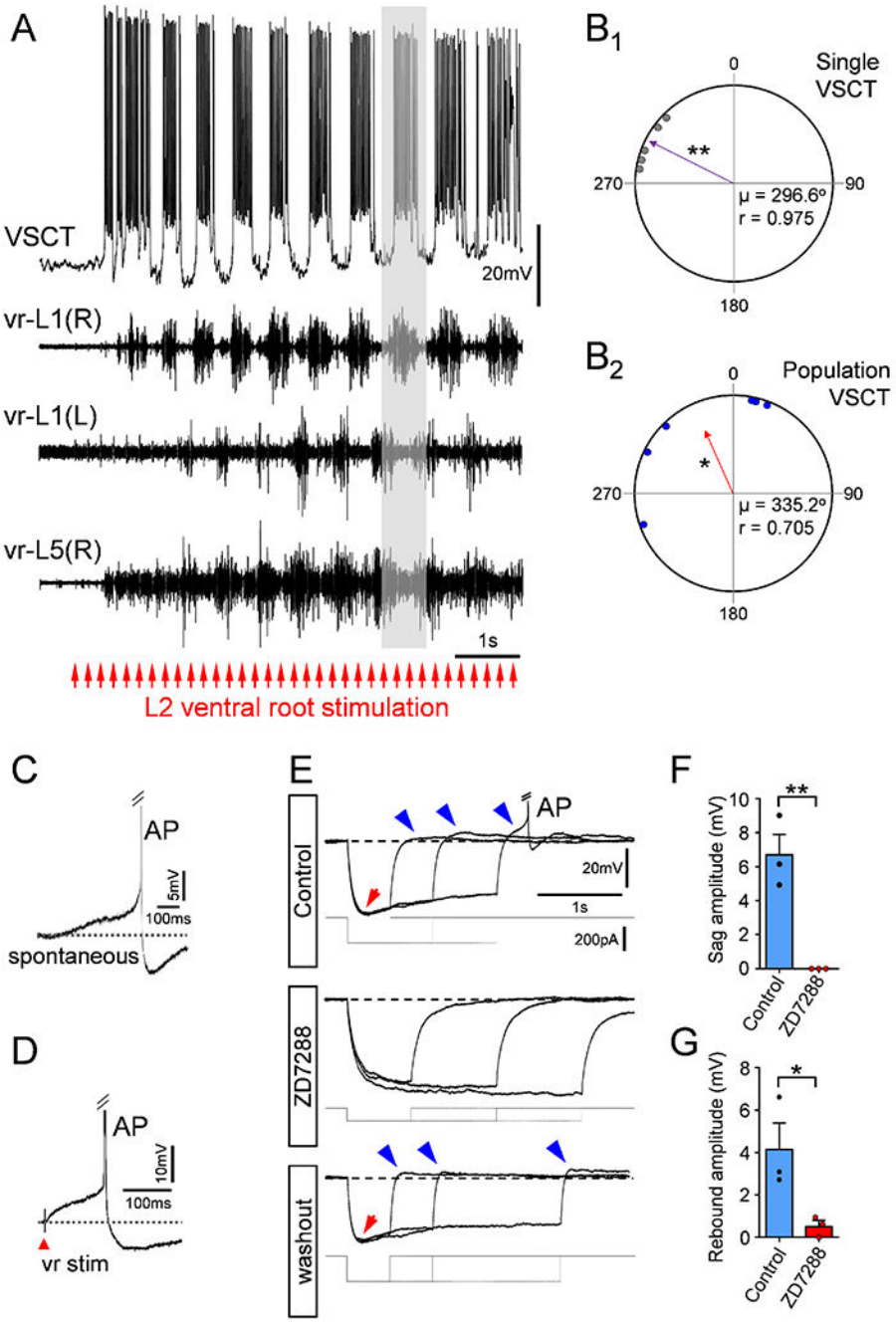

Figure 3. VSCTs are rhythmic during locomotor behavior and exhibit rhythmogenic properties.

(**A**) Rhythmic activity in a P4 L1 VSCT together with filtered extracellular traces from ipsilateral (R) and contralateral (L) homosegmental L1 VRs and L5 (R) VR during locomotor-like activity induced by electrical stimulation of VR-L2 (bottom red arrows; 5Hz for 10s). Stimulus artifacts have been removed for clarity (n=6 VSCTs, N=6 mice). (**B_1**) Quantification of timing of first AP in a single VSCT with respect to the locomotor cycle in the homosegmental VR. Purple arrow vector indicates that the VSCT exhibited significant rhythmicity and fired prior to the onset of MN activity. ** p<0.01, Rayleigh

Test. (**B_2**) Quantification of timing of firing for the population of VSCTs to the locomotor cycle. Each data point represents the rhythmic vector value from individual VSCTs (purple arrow in B_1). Red arrow vector indicates that the population of VSCTs exhibit rhythmic activity preceding MN activity. * $p<0.05$, Rayleigh Test, μ: mean vector; r: length of the mean vector. VSCTs exhibit characteristics of a pacemaker current both spontaneously (**C**) and evoked after VR stimulation (**D**) (n=6, N=6). (**E**) Superimposed voltage responses from a P4 L2 VSCT exhibiting a sag (red arrow) and post-inhibitory rebound (blue arrows) after negative current injection (bottom traces). Truncated AP is shown in **E**. ZD7288 (100μM) abolished both sag and post-inhibitory rebound and recovered after washout. Sag (**F**) and post-inhibitory rebound (**G**) amplitude before and after ZD7288 in 3 VSCTs. * $p<0.05$, ** $p<0.01$; Two-tailed student's t-test. Data are represented as mean ± SEM. See also Fig. S3.

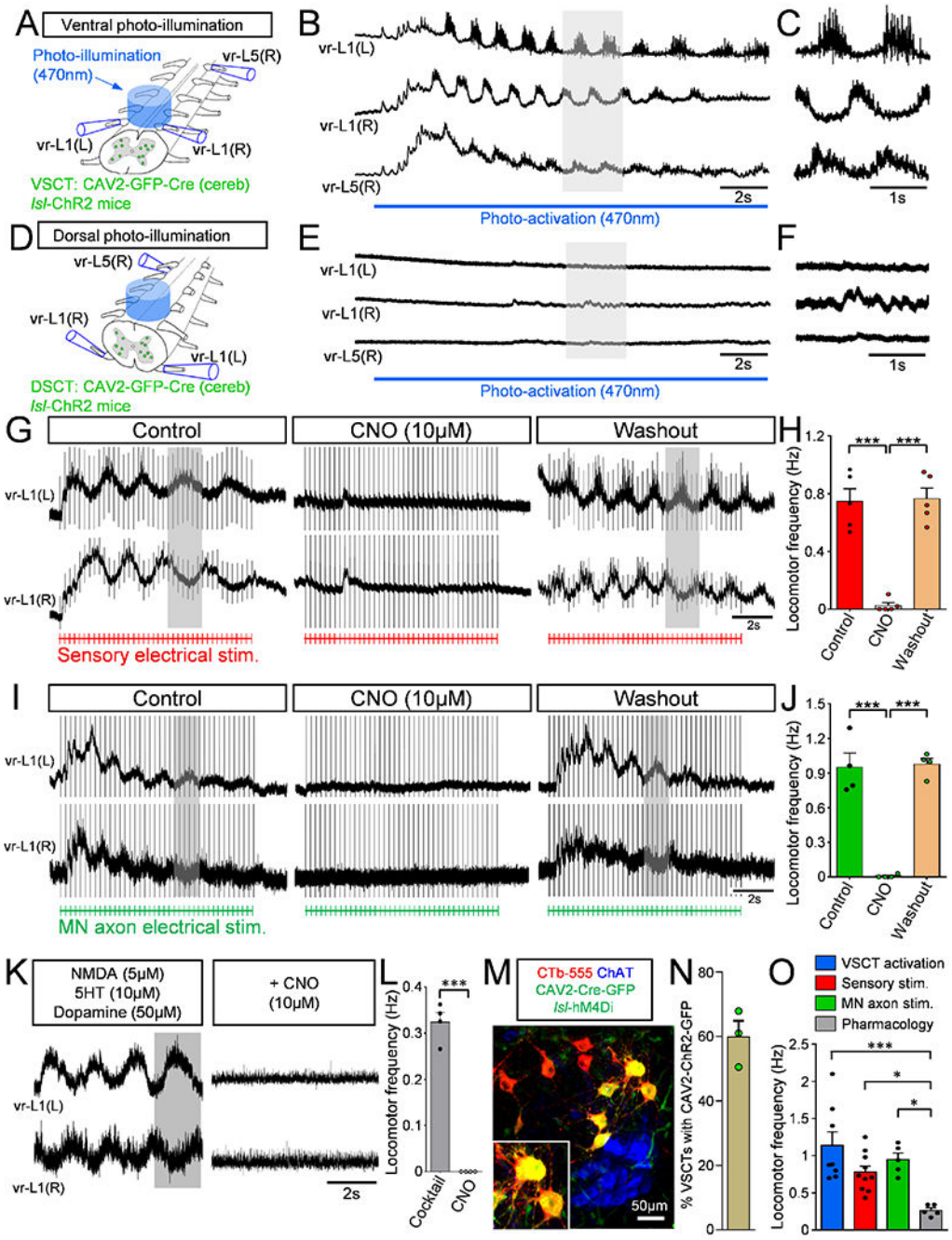

Figure 4. VSCTs are necessary and sufficient for locomotor-like behavior.

(**A**) Bilateral illumination with a 470nm LED from the ventral aspect of L1 and L2 segments resulting in locomotor behavior recorded from L1 and L5 VRs (**B**) in *ex vivo* spinal cord at P4. (**C**) Expanded traces (grey box in **B**) showing alternating activity between VRs (N=8). (**D**) Bilateral photoactivation of the dorsal aspect of the L1/L2 spinal cord. (**E**) Extracellular VR responses following dorsal photo-activation (same spinal cord as in **B** but flipped over 180°). (F) Time-expanded traces (grey box in **E**). (**G**) Locomotor behavior evoked by sensory stimulation before, during and after CNO washout in a spinal cord

expressing hM4Di in VSCTs (duration of stimulation: red drawing at the bottom, 4Hz for 10s). (**H**) Locomotor frequency after sensory stimulation before, during CNO and after washout (N=5). (Control vs. CNO: *** p<0.001; CNO vs. Washout: *** p<0.001, One Way ANOVA, Tukey's *post hoc* test). (**I**) As in (**G**), locomotor behavior induced following VR stimulation (bottom in green, 5Hz for 10s) before, during and after CNO application. (**J**) Locomotor frequency following MN axon stimulation before, during and after CNO (N=4). (Control vs. CNO: *** p<0.001; CNO vs. Washout: *** p<0.001, One Way ANOVA, Tukey's *post hoc* test). (**K**) Similar to (**G**) and (**I**), VR responses in which locomotor activity was induced by application of NMDA (5μM), 5HT (10μM) and dopamine (50μM). Exposure to CNO abolished locomotor activity. (**L**) Locomotor frequency evoked by pharmacological activation, before and after CNO application (N=4). *** p<0.001, Two-tailed student's t-test. (**M**) Confocal image showing MNs (ChAT, blue), VSCTs (CTb-555, red) and CAV2-Cre-GFP (green) in a/*s*/-hM4Di mouse. (**N**) Percentage of VSCTs transduced with CAV2-GFP at P5 (N=3). (**O**) Locomotor frequency under photoactivation of VSCTs (blue), sensory (red) and MN stimulation (green), and cocktail of drugs (grey). (VSCT v Pharmacology: *** p<0.001; Sensory v Pharmacology, * p<0.05; MN axon v Pharmacology, * p<0.05, One Way ANOVA, Tukey's *post hoc* test). Data are represented as mean ± SEM. See also Figs. S4 and S5.

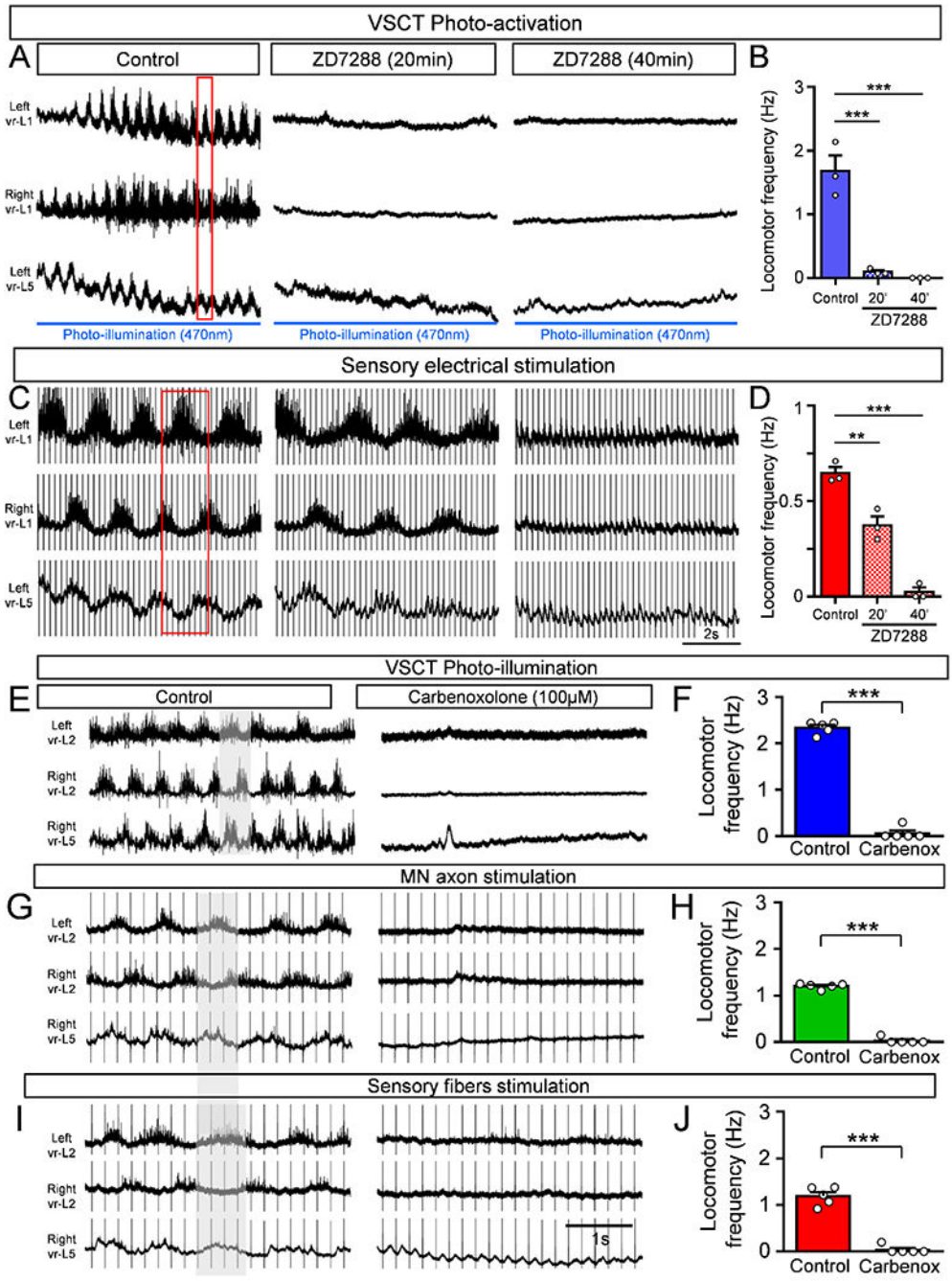

Figure 5. The locomotor activity induced after photo-activation of VSCTs depends upon the h-current and gap junctions.

(**A**) Locomotor-like behavior induced by photo-illumination of VSCTs expressing ChR2 at P4 under control aCSF, and its abolition 20min and 40min after 100µM ZD7288 application. Duration of photoactivation: blue line. Red box: alternating activity in VRs. (**B**) Locomotor frequency before, 20min and 40min after ZD7288 (N=3). (**C**) Locomotor activity induced by sensory electrical stimulation in the same spinal cord shown in (**A**). Exposure to ZD7288 reduced locomotor activity after 20min and abolished it after 40min.

(**D**) Locomotor frequency before, 20min and 40min after ZD7288. ** p<0.01, *** p<0.001, One Way ANOVA, Tukey's *post hoc* test for both **B** and **D**. Locomotor activity induced by VSCT photoactivation in the L4/L5 segments from P3-P4 mice (**E**) or MN axon (vr-L5 L) stimulation (**G**) or sensory fiber (dr-L5 L) stimulation (**I**) in the same spinal cord. Carbenoxolone (100μM) abolished locomotor activity in all cases. Locomotor frequency following photo-activation of VSCTs (**F**), MN axon stimulation (**H**) and sensory fiber stimulation (**J**), before and after carbenoxolone. *** p<0.001, Two tailed, unpaired t-test (N=5). Data are represented as mean ± SEM. See also Fig. S5.

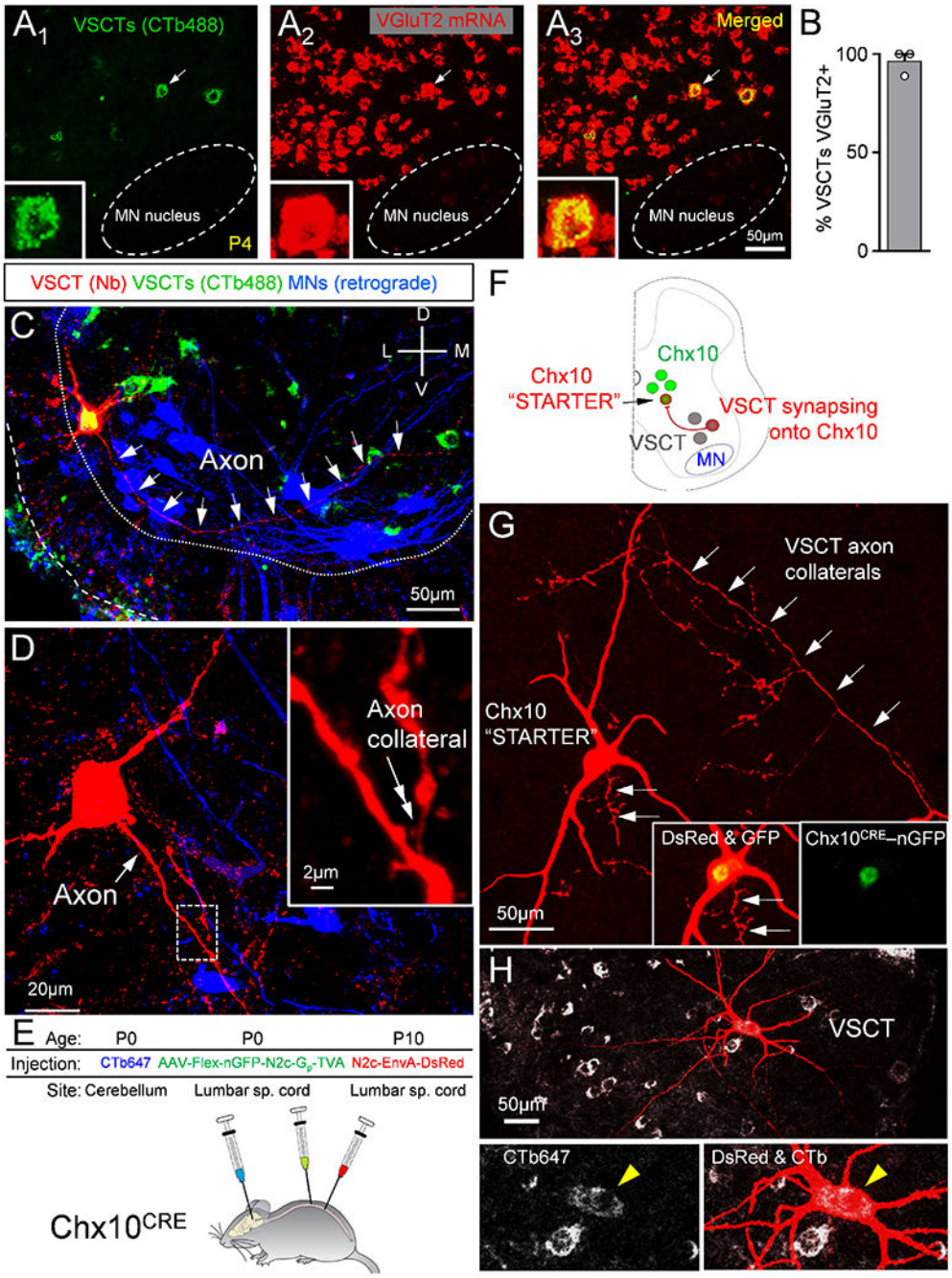

Figure 6. VSCTs are glutamatergic, possess spinal axon collaterals and make synapses with Chx10 spinal neurons.

(**A**$_{1\text{-}3}$) VSCTs (CTb-488 from cerebellum, green) and VGluT2 mRNA (red) and merged image. Inset: VSCT (arrow in A$_{1\text{-}3}$) expressing VGluT2. (**B**) Percentage of VSCTs expressing VGluT2 (N=3). (**C**) A P4 L2 VSCT filled with Neurobiotin (red) after intracellular recording colocalizing with CTb-488 (cerebellum at P0). MNs were backfilled with a dextran dye from the VR (blue). White arrows mark VSCT axon. (**D**) Higher mag of VSCT [in (**C**)], showing its main axon (white arrow) and an ipsilaterally projecting

axon collateral (inset, double arrow; magnified from the dotted box). (**E**) AAV2/1-Flex-nGFP-N2c-Gp-TVA injected in spinal cord at P0 to introduce the rabies G protein to Chx10 neurons ($Chx10^{CRE}$ mice). Concurrently, CTb-647 injected in cerebellum to mark VSCTs. Rabies-N2c-EnvA-dsRed was injected in spinal cord at P10. (**F**) The "starter" Chx10 neurons are labeled with nuclear GFP and cytoplasmic dsRed. Neurons providing monosynaptic input to "starter" neurons are labeled with dsRed, but not nGFP. VSCTs are identified through CTb647. (**G**) A Chx10 "starter" neuron identified by co-localization of dsRed and nGFP (insets). Arrows indicate VSCT axon collaterals synapsing onto the Chx10 "starter" neuron. (**H**) VSCT (yellow arrowhead in insets) labeled by transynaptic transfection of its axon collaterals onto the Chx10 neuron. Data are represented as mean ± SEM. See also Figs. S6 and S7.

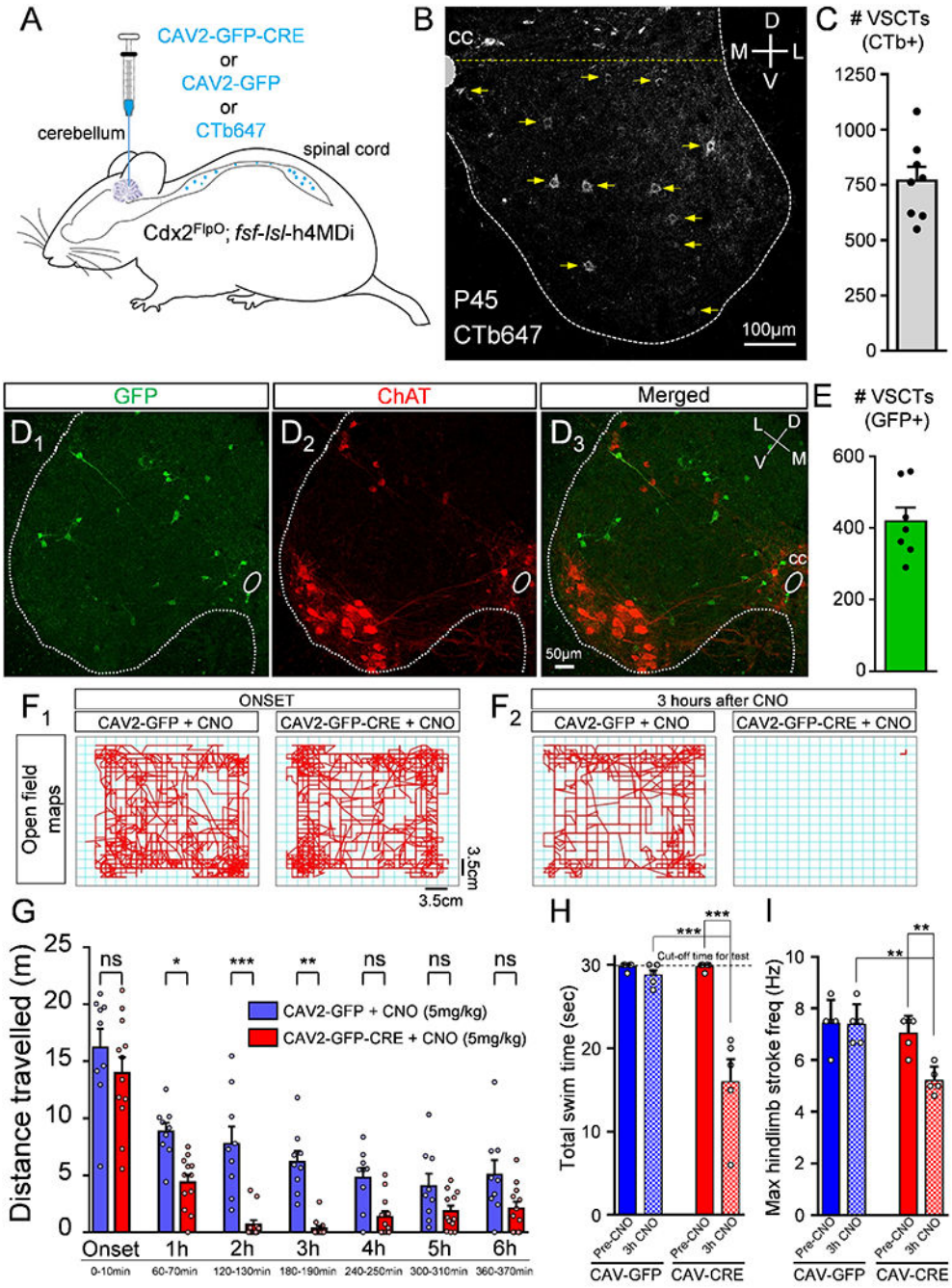

Figure 7. Silencing VSCTs *in vivo* in freely-moving adult mice perturbs locomotor ability.

(**A**) CAV2-GFP-CRE or CAV2-GFP or CTb647 (for counting) was injected in cerebellum at ~P21 in Cdx2^{Flpo}::*fsf-lsl*-h4MDi mice. (**B**) CTb647+ neurons in the L1 segment in a P45 mouse. Neurons ventral to the yellow dotted line were defined as VSCTs. (**C**) Total number of VSCTs labelled with CTb647 in the L1 segment (N=8). GFP in the L1 segment (**D_1**: green), ChAT (**D_2**: red) and merged image (**D_3**). (**E**) Total number of GFP+ VSCTs in mice injected with CAV2-GFP-CRE (N=7). Maps of distance travelled by a mouse in open field assay in 10mins at the onset (**F_1**) and after 3hours (**F_2**) for each group (age: P45). (**G**)

Distance travelled by mice in bins of 10mins duration for each hour after CNO injection (N=9 CAV2-GFP mice, blue; and N=12 CAV2-GFP-CRE mice, red). Each point represents a single mouse, ns: no significance ($p>0.05$), * $p<0.05$, *** $p<0.001$, One WayANOVA, Tukey's *post hoc* test. (**H**) Total swim time for control (CAV2-GFP; blue) and CAV2-CRE (red) mice, before (Pre-CNO) and 3 hours after 10mg/kg CNO (3h CNO). (**I**) Maximum hindlimb stroke frequency during periods of swimming for the two groups. ** $p<0.01$, *** $p<0.001$, One Way ANOVA, Tukey's post hoc test for both H and I. Data are represented as mean ± SEM. See also Figs. S8 and S9 and Videos 1, 2 and 3.